Study of the Bose-Einstein correlations of same-sign pions in proton-lead collisions

LHCb collaboration[†]

Abstract

Correlations of same-sign charged particles are analysed using proton-lead collision data collected by the LHCb experiment at a nucleon-nucleon centre-of-mass energy of 5.02 TeV, corresponding to an integrated luminosity of 1.06 nb^{-1}. Bose-Einstein correlations are observed in the form of an enhancement of pair production for same-sign charged pions with a small four-momentum difference squared. The dependence of the correlation radius and the intercept parameter on the reconstructed charged-particle multiplicity is investigated. The measured correlation radii scale linearly with the cube root of the reconstructed charged-particle multiplicity, being compatible with predictions of hydrodynamic models on the collision system evolution.

[†]Authors are listed at the end of this paper.

1 Introduction

Multiparticle production in the process of hadronization has been investigated for six decades but its nature is still not fully understood. The Hanbury Brown-Twiss (HBT) intensity interferometry [1–3] is the main tool to study the space-time properties of the hadron emission volume. In the case of joint production of identical bosons the HBT interference effect results in Bose-Einstein Correlations (BEC), while in the case of fermions it is referred to as Fermi-Dirac Correlations (FDC). The correlations measure the scales that are referred to as lengths of homogeneity [4,5], which correspond to a limited region of the particle-emitting source surface. Measurement of correlations of identical particles can provide insight into the evolution of the hadron source. In particular, small systems, such as those produced in proton-ion (pA) collisions, are interesting because their lifetimes are significantly shorter than those in heavy-ion (AA) collisions, thus providing a better probe of the early system dynamics and the initial geometry.

Since the first observation of quantum interference effects in identically charged pions produced in proton-antiproton collisions [6], such effects have been investigated by many different experiments, *e.g.* at the Berkeley Bevalac [7], AGS [8], ISR [9–11], SPS [12–14], LEP [15–30], RHIC [31–43], LHC [44–62] and others [63,64]. The sizes of the studied systems vary tremendously, from e^+e^- collisions at LEP to AuAu collisions at RHIC and PbPb beams at LHC. At the LHC alone, the HBT effect has been investigated in proton-proton (pp) [44–57], proton-lead (pPb) [54–60] and lead-lead (PbPb) [53–56,60–62] systems.

In this paper, the first study of the BEC effect in pPb and Pbp collisions in the forward rapidity region is presented. The LHCb detector has the potential to measure quantum interference effects in the forward region, and therefore to provide complementary results to those from experiments at the LHC in the central rapidity region. This allows to study the dependence of the quantum interference effects upon various observables, and it provides insight into the particle production process in the forward direction, useful for the development of theoretical models.

2 Analysis method

The BEC or FDC effects are the result of the quantum statistics, caused by the symmetrization (antisymmetrization) of the wave function describing a system of bosons (fermions). Such correlations are examined by measuring a two-particle correlation function, defined as the ratio of the inclusive density distribution for two particles and the so-called reference density. The latter is a two-particle density distribution that approximates the distribution without the BEC or FDC effects. The present study is based on the assumption of static, spherically-symmetric sources that can be characterized by univariate distributions. This class of sources is commonly used in HBT analyses, since the measured correlation radii in this case can be interpreted as the effective size of the particle-emitting source at the kinetic freeze-out [65,66].

2.1 Correlation function

In order to investigate the space-time evolution of the hadronization source, the correlation function is commonly studied using the Lorentz-invariant variable Q [67], which is related

to the difference in the four-momenta q_1 and q_2 of two indistinguishable particles of rest mass m,

$$Q \equiv \sqrt{-(q_1 - q_2)^2} = \sqrt{M^2 - 4m^2} \ . \tag{1}$$

This gives a measure of the phase-space separation of the two-particle system of invariant mass M. A two-particle correlation function C_2 is constructed as the ratio of the Q distributions for signal and reference pairs

$$C_2(Q) = \left(\frac{N^{\text{ref}}}{N^{\text{sig}}}\right) \left(\frac{\mathrm{d}N^{\text{sig}}(Q)\,/\,\mathrm{d}Q}{\mathrm{d}N^{\text{ref}}(Q)\,/\,\mathrm{d}Q}\right) \ , \tag{2}$$

where N^{sig} and N^{ref} correspond to the number of signal and reference pairs, respectively, obtained from an integral of the relevant Q distributions. Signal pairs are formed from selected same-sign (SS) charged particles that originate from the same collision vertex where the Bose-Einstein correlations are expected. The reference pairs are pairs of pions which reproduce as closely as possible the kinematics and various effects present in the signal, except for the BEC effect. The correlation function is constructed as a ratio to cancel the effects related to the detection efficiency.

There are several methods to obtain a reference sample. It can be constructed using experimental data, or with simulated events incorporating the detector interactions. In this study, a data-driven reference sample is constructed by collecting pairs of particles originating from different collision events (a so-called event-mixing method), where the BEC effect cannot be present. The reference pairs are selected in the similar way as the signal ones to ensure that the signal kinematic distributions are reproduced as closely as possible. Additional requirements are imposed to combine particles originating from different events with similar properties and to further improve the agreement between the signal and reference samples. Particles in the reference pairs are required to originate from primary vertices with a comparable multiplicity of tracks reconstructed in the vertex detector (VELO tracks). Event-mixing candidates for the current event are provided by creating a pool of selected particles from ten different events and splitting them into intervals of multiplicity and the coordinate of the PV along the beam direction z_{PV}. Then, for each signal pair in a PV with a given (multiplicity, z_{PV}) interval, a random particle is chosen from the relevant interval in the pool to create a reference pair with the particle in the signal pair. Candidate particles to create pairs are grouped into multiplicity bins of width of three. The distance between the two PVs associated with the two particles in the same reference pair must be smaller than 10 mm in the z direction to provide consistent detector acceptance effects for both particles.

The two-particle correlation function associated with a general class of particle sources can be described by the so-called symmetric Lévy-stable distributions [68]. In the case of static, univariate sources, the Lévy-type correlation function is expressed as

$$C_{2,\text{BEC}}(Q) = 1 + e^{-|RQ|^{\alpha_L}} \ , \tag{3}$$

where R denotes the correlation radius, and α_L is a parameter that can take values in the range $0 < \alpha_L < 2$ and is referred to as a Lévy index of stability. Frequently, to enable comparison of the correlation parameters between experiments and between different collision systems, including a measurement by LHCb in pp collisions [52], α_L is fixed to one, leading to the simplified expression:

$$C_{2,\text{BEC}}(Q) = 1 + e^{-|RQ|} \ . \tag{4}$$

This parametrization enables the measured correlation radius to be interpreted as the effective size of the particle-emitting source.

2.2 Final state interactions and nonfemtoscopic effects

Final state interactions (FSI) resulting from the strong and electromagnetic forces can affect the observed two-particle correlations. The effects of the strong interaction in the case of pions is relatively small [69] and is usually neglected in BEC studies. The most notable effect is Coulomb repulsion related to the same-sign electric charge of the studied particles, especially in the low-Q region. A general expression for the Coulomb interaction term for point-like sources [69–71], $K(Q)$, is equivalent to the so-called Gamov factor [72]

$$K_{\text{Gamov}}^{\text{SS}}(\zeta) = \frac{2\pi\zeta}{e^{2\pi\zeta} - 1} \ , \ K_{\text{Gamov}}^{\text{OS}}(\zeta) = \frac{2\pi\zeta}{1 - e^{-2\pi\zeta}} \ , \tag{5}$$

where $\zeta = \alpha m / Q$, α is the fine-structure constant and m is the particle's rest mass. For SS particles, a repulsive interaction leads to a decrease in the correlation function, which is most prominent for low Q-values. In the case of opposite-sign (OS) pairs, this effect is reversed and an enhancement is observed. The OS sample is useful to parametrize the background related to the cluster contribution, as explained later.

In the present analysis a parametrization developed by the CMS experiment [56], valid for the Lévy-type sources with α_L equal to unity, is used to account for the final-state Coulomb interactions between the particles in the SS and OS pairs

$$K(Q) = K_{\text{Gamov}}(Q) \left(1 + \frac{\alpha\pi m R_{\text{eff}}}{1.26 + Q R_{\text{eff}}} \right) \ , \tag{6}$$

where R_{eff} corresponds to the effective size of the particle-emitting source and is provided in femtometres. The additional term with R_{eff} represents a correction to the Gamov factor that enables a more precise characterization of the Coulomb interaction for extended sources.

The correlation function shape is distorted by the presence of various nonfemtoscopic[1] effects. There is no strict, theory-motivated description of such contributions, and different strategies can be applied to take them into account in the analysis (see Sec. 5). Long-range correlations, being one of nonfemtoscopic effects related mostly to the energy-momentum conservation, are present in the full Q range, but are most prominent at the high-Q values ($\sim Q > 1\,\text{GeV}$)[2], far from the BEC-signal region. Although different parametrizations can be employed, a simple term linear in Q is usually optimal to characterize this contribution and is therefore commonly used [73, 74].

Cluster contribution [56] is another prominent component of the nonfemtoscopic background, related to the effects of particles emitted inside low-momentum mini-jets and multibody decays of resonances. It is difficult to correct for the long-range correlations, as these are present dominantly in the range $Q < 0.5$–1.0 GeV that overlaps with the BEC signal. Constructing a correlation function for OS pairs can be particularly useful in the background studies, since similar effects can be expected for both the SS and OS pairs. Special care must be taken when investigating OS pairs, due to structures related to two-body decays of resonances, arising in the correlation function.

---

[1]Femtoscopic effects are those observed at the Fermi scale.
[2]If not indicated otherwise natural units with $c = 1$ are used.

Nonfemtoscopic background effects in the present analysis (in particular the cluster contribution) are studied and parametrized using the OS correlation functions. A cluster subtraction (CS) method, which was developed by the CMS experiment [46,56], is employed for this purpose. This technique represents a fully data-driven approach. In the CS method, the shape parameters of the chosen function for the background description (e.g. the width of a Gaussian distribution) are determined from the OS fits. The background shape parameters in the SS fits are fixed to the values determined by studying the OS pairs, with an additional scaling parameter that is introduced to account for the different amplitudes of the cluster contribution in the SS and OS correlation functions.

2.3 Fitting method

The correlation function, including electromagnetic effects and the nonfemoscopic background, is parameterized using the Bowler–Sinyukov formalism [69,70], as

$$C_2(Q) = N \left[1 - \lambda + \lambda K(Q) \times \left(1 + e^{-|RQ|} \right) \right] \times \Omega(Q) , \qquad (7)$$

where N is a normalization factor and $\Omega(Q)$ is a general term for the nonfemtoscopic background contribution, as described later. The intercept parameter, λ, corresponds to the extrapolated value of the correlation function at $Q = 0$ GeV [65]. This observable can be interpreted within the core-halo model [75], which assumes that the particle emission can take place in a central core or in an extended halo originating from long-lived resonance decays.

Contents of the bins in both the signal and reference Q-variable histograms are Poisson-distributed, and hence a negative log-likelihood fit method is preferable for the BEC studies [8,59]. In this approach, the following expression is minimized in the fitting procedure:

$$-2 \ln L = 2 \sum_i \left\{ A_i \ln \left[\frac{(1 + C_{2i}) A_i}{C_{2i} (A_i + B_i + 2)} \right] + (B_i + 2) \ln \left[\frac{(1 + C_{2i}) (B_i + 2)}{A_i + B_i + 2} \right] \right\} , \qquad (8)$$

where A_i and B_i are the bin contents of the signal and reference Q histograms and C_{2i} corresponds to the fitted value of the correlation function at the Q-bin centre.

3 Detector and dataset

The LHCb detector [76,77] is a single-arm forward spectrometer covering the pseudorapidity range $2 < \eta < 5$, designed for the study of particles containing b or c quarks. The detector includes a high-precision tracking system consisting of a silicon-strip vertex detector (VELO) surrounding the interaction region [78], a large-area silicon-strip detector located upstream of a dipole magnet with a bending power of about $4\,\mathrm{Tm}$, and three stations of silicon-strip detectors and straw drift tubes [79] placed downstream of the magnet. The tracking system provides a measurement of the momentum, p, of charged particles with a relative uncertainty that varies from 0.5% at low momentum to 1.0% at 200 GeV. The minimum distance of a track to a primary collision vertex (PV), the impact parameter, is measured with a resolution of $(15 + 29/\, p_{\mathrm{T}})\ \mu\mathrm{m}$, where p_{T} is the component of the momentum transverse to the beam, in GeV. Different types of charged hadrons are

distinguished using information from two ring-imaging Cherenkov detectors [80]. Photons, electrons and hadrons are identified by a calorimeter system consisting of scintillating-pad and preshower detectors, an electromagnetic and a hadronic calorimeter. Muons are identified by a system composed of alternating layers of iron and multiwire proportional chambers [81]. The trigger [82] consists of a hardware stage, based on information from the calorimeter and muon systems, followed by a software stage, which applies a full event reconstruction.

In the present analysis, a dataset of minimum-bias triggered events collected in pPb collisions recorded in 2013 at a nucleon-nucleon centre-of-mass energy $\sqrt{s_{\mathrm{NN}}} = 5.02$ TeV is used, with 4 and 1.58 TeV beam energies, respectively. Two collision modes were used in this data-taking period with the beam directions reversed, which permits the study of pPb collisions both in the forward and backward rapidity regions. The recorded pPb and Pbp samples correspond to integrated luminosities of 1.06 nb^{-1} and 0.52 nb^{-1}, respectively. As only a fraction of $\sim 10^{-5}$ of the collisions corresponds to multiple interactions, a dedicated selection requirement is applied to accept only the events with a single primary vertex. The data samples available in the current study after selection described in Sec. 4 corresponds to $\sim 6.3 \times 10^7$ (5.7×10^7) events for the pPb (Pbp) collisions.

Simulation samples corresponding to the 2013 pPb data-taking conditions are produced using the EPOS [83] generator, with a specific LHCb configuration [84]. Decays of hadronic particles are described by EvtGen [85], in which final-state radiation is generated using Photos [86]. The interaction of the generated particles with the detector and its response are implemented using the Geant4 toolkit [87,88], as described in [89]. The BEC effect is not activated in the simulation. Each of the pPb and Pbp simulated dataset contains $\sim 1.2 \times 10^7$ events after selection, with the number of interactions per bunch crossing fixed to unity. The simulation samples are used mainly for the event-selection optimization, while the background modelling is performed with a purely data-driven approach.

4 Event selection

The data samples are divided into bins of the multiplicity of VELO tracks assigned to a PV (N_{VELO}), which is used as a proxy variable to describe the total charged-particle multiplicity produced at the PV. The division is optimized to obtain a high number of bins with enough entries to perform the measurement (see appendix A). The chosen binning scheme is presented in Table 1, together with approximate fractions of the respective sample corresponding to the given bin.

Event selections are first applied to single-pion candidates. All pion candidates must have reconstructed track segments in both the VELO detector and tracking stations downstream of the magnet, have no matching tracks in the muon stations, and be in the pseudorapidity range $2 < \eta < 5$. Each track must have a good track-fit quality and $p_{\mathrm{T}} > 0.1$ GeV. To suppress the contribution from secondary pions (those not associated to a PV), the impact parameter is required to be less than 0.4 mm. Furthermore, the PV is required to be located within $-160 < z_{\mathrm{PV}} < 60$ mm.

The particle identification (PID) is based on the output of a neural network employing subdetector information that quantifies the probability ProbNN for a particle to be of a certain kind [80]. The simulated quantities are corrected using PID calibration samples in data [90]. Effects of PID correlations between particles are considered. It is important to

Table 1: Ranges of the VELO-track multiplicity bins in the pPb and Pbp datasets. An approximate fraction of the relevant data sample corresponding to the given bin is also indicated.

bin#	N_{VELO}	Sample fraction [%] pPb	Sample fraction [%] Pbp
1	5–9	< 2	< 2
2	10–14	2	2
3	15–19	4	2
4	20–24	7	3
5	25–29	10	4
6	30–34	13	5
7	35–39	14	6
8	40–44	10	5
9	45–49	10	6
10	50–54	8	6
11	55–59	7	7
12	60–64	5	6
13	65–79	6	15
14	80–89	–	7
15	90–99	–	7
16	100–114	–	6
17	115–139	–	7
18	140–179	–	4

ensure a sample with high purity, but a strict requirement on ProbNN(π) variable may also strongly affect the signal region of the correlation function, by suppressing low-momentum pions that contribute to the BEC effect. The nominal requirement of ProbNN(π) > 0.65 is imposed to make this analysis consistent with the previous analysis for pp collisions [52]. Varying this requirement from 0.5 to 0.8 shows no significant changes in the measured correlation function.

Contamination from incorrectly reconstructed particles can influence the measured Bose-Einstein correlations effect. Cloned tracks, being multiple tracks reconstructed from hits that were deposited by a single charged particle, are especially detrimental as they are present mostly in the low-Q region ($Q < 1.0\,\mathrm{GeV}$), where the BEC signal is expected, appearing as a pair of almost identical, seemingly correlated, particles. To control this effect, the slopes of the track are studied. The cloned tracks usually share a very similar trajectory, hence the differences in the relevant slopes in a particle pair ($\Delta t_x = p_{x_1}/p_{z_1} - p_{x_2}/p_{z_2}$ and $\Delta t_y = p_{y_1}/p_{z_1} - p_{y_2}/p_{z_2}$) tend to be small. A requirement is imposed to limit this contribution, $i.e.$ if both $|\Delta t_x|$ and $|\Delta t_y|$ values are smaller than 0.3×10^{-3}, then the pair is discarded. After applying these requirements, the effect of the clone particles is found to be negligible in the region $Q > 0.05$ GeV. In order to further reduce the contamination from cloned tracks and fake tracks (which do not correspond to any particle trajectory, but are reconstructed from a number of unrelated hits), in the case where the tracks share all the same hits deposited in the VELO subdetector, only the track with the best χ^2/ndf is retained.

The study of the correlations is limited to the Q range from 0.05 to 2.0 GeV. In the region with very low Q (< 0.05 GeV) the separation in the momentum between the particles is poor and the discrepancy between simulation and data grows as Q vanishes. Furthermore, investigations using simulation indicate that there is a significant fraction of pion pairs containing fake tracks and cloned tracks in the region $Q < 0.05$ GeV for all multiplicity bins.

5 Fitting correlation functions

Correlation functions for both the SS and OS pairs are constructed for Q values between 0.05-2.0 GeV with a bin width of 0.005 GeV. This particular choice enhances consistency with the study performed for pp collisions [52] and allows a direct comparison of the results of the two analyses. The correlation function for the SS pairs is studied by fitting the Q spectrum using Eq. 7. The effective radius R_{eff} in Eq. 6 is set to 2 fm, based on the expected correlation radii. The description of nonfemtoscopic background effects is found using the correlation function for the OS pairs. The resulting contribution is then scaled and fixed in the final fits to the SS correlation functions, as explained in detail below.

The presence of structures related to intermediate states, such as $\rho^0(770)$, $K_{\text{S}}^0(497)$, $f_0(980)$, $f_2(1270)$, in the OS correlation functions degrades the quality of the fit from which the nonfemtoscopic background parameters are determined. Therefore, the affected regions are removed from the fit to the correlation function. The boundaries of the removed regions are optimized to provide a good quality of fits to the correlation function for OS pairs, and the choice of particular boundary values is accounted for in the study of the systematic uncertainties. It is worth noting that the impact of resonances is most prominent in the bins with low N_{VELO} values. The observed structures quickly diminish with increasing multiplicity due to a prevailing contribution from pairs of unrelated particles.

As it has been already mentioned, the OS correlation functions contain similar effects as the SS ones (apart from the BEC signal) and can be used to investigate the nonfemtoscopic background contribution. A satisfactory description of the data is found using a Gaussian parametrization for the cluster contribution [56]

$$\Omega(Q) = (1 + \delta Q) \times \left[1 + z \frac{A_{\text{bkg}}}{\sigma_{\text{bkg}} \sqrt{2\pi}} \exp\left(-\frac{Q^2}{2\sigma_{\text{bkg}}^2} \right) \right] , \qquad (9)$$

where the term linear in δ corresponds to the long-range correlations and the z parameter (fixed to unity in the OS fits) is a factor used for the background scaling between OS and SS pairs. The width σ_{bkg} and amplitude A_{bkg} are multiplicity-dependent values that characterize the cluster contribution and are parametrized as [46, 56]

$$\sigma_{\text{bkg}}(N_{\text{VELO}}) = \sigma_0 + \sigma_1 \exp\left(-\frac{N_{\text{VELO}}}{N_0} \right) , \qquad (10)$$

$$A_{\text{bkg}}(N_{\text{VELO}}) = \frac{A_0}{(N_{\text{VELO}})^{n_A}} . \qquad (11)$$

The fits to the correlation functions for OS pairs are performed simultaneously in all multiplicity bins available in the given sample (separately for the pPb and Pbp datasets).
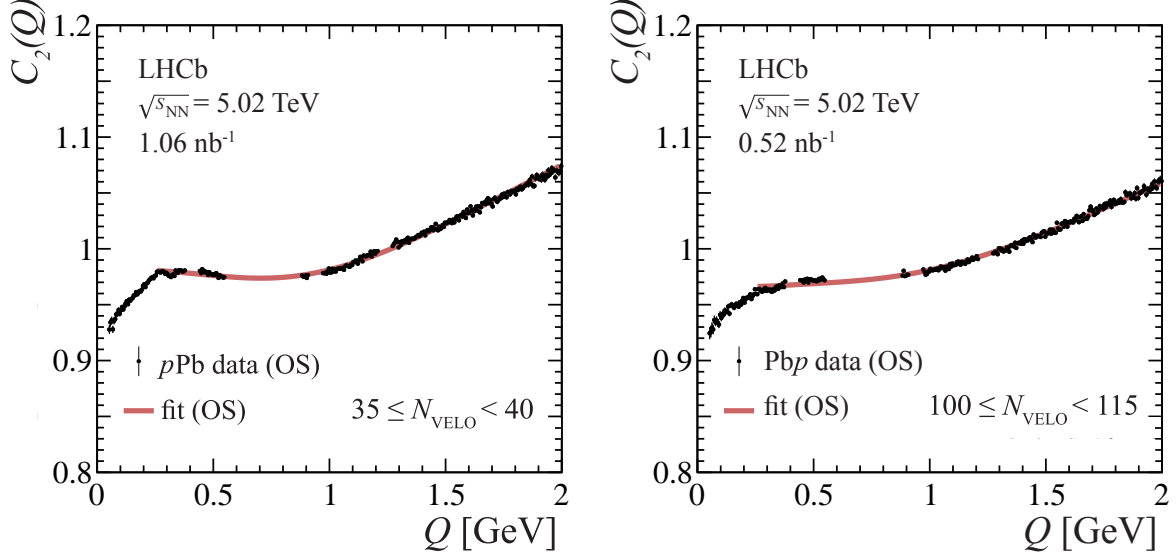
Figure 1: Example of the OS correlation functions in individual N_{VELO} bins together with the global fit using Eq. 9 to parametrize the cluster contribution. The results are shown for (left) a moderate-multiplicity region ($35 \leqslant N_{\text{VELO}} < 40$) of the pPb and (right) a high-multiplicity regime ($100 \leqslant N_{\text{VELO}} < 115$) of the Pb$p$ dataset. Only statistical uncertainties are shown.

In this procedure, the parameters from Eqs. 10 and 11 are common for all bins, while the N and δ values (Eqs. 7 and 9 respectively) are left free for each correlation function. A negative log-likelihood function (see Eq. 8) is constructed for all the N_{VELO} bins in the given dataset and minimized globally to obtain the best description of the data. The lower Q fit range for the OS pairs is limited with respect to the SS ones, due to a significant contribution of multibody resonance decays in the very low Q region [46, 59]. The global fits are performed for $Q > 0.25$ GeV. Also, as it is found that the best stability of the global fits is obtained with a fixed value of the N_0 parameter from Eq. 10, its value is set to 15 based on the fit results for the entire pPb dataset obtained with this parameter left free. Results of the global fits to the OS correlation functions for the pPb and Pbp data are shown in Fig. 1 and summarized in Table 2. The quality of the fits is evaluated through the normalized Baker-Cousin likelihood ratio corresponding to the final value of the function minimized in the fitting procedure (see Eq. 8), divided by the number of degrees of freedom in the fit ($\sim$2 for both pPb and Pbp). It is worth noting that the fit quality in BEC studies is not expected to be perfect. Due to the ad hoc descriptions of the unknown nonfemtoscopic background contribution as well as the compromise between the fit quality and interpretability of the measured correlation parameters, the obtained χ^2/ndf values are often larger than unity.

The cluster contribution is expected to be larger for the OS pairs than for the SS ones due to the charge conservation in processes contributing to the cluster formation. For this reason, the amplitude of the cluster contribution for the SS correlation functions is multiplied by the scaling factor z (see Eq. 9). To obtain a uniform background scaling across the N_{VELO}, this value is parametrized using a theoretically motivated form based

Table 2: Results of the global fits to the OS correlation functions using Eq. 9 to parametrize the cluster contribution in the pPb and Pbp data.

Dataset	A_0 [GeV]	n_A	σ_0 [GeV]	σ_1 [GeV]
pPb	2.838 ± 0.109	0.8438 ± 0.0111	0.4799 ± 0.0018	0.1744 ± 0.0060
Pbp	1.107 ± 0.022	0.5036 ± 0.0049	0.5613 ± 0.0013	0.0 ± 10^{-3}

on the ratio of SS and OS pair combinatorics [56]

$$z(N_{\mathrm{VELO}}) = \frac{aN_{\mathrm{VELO}} + b}{1 + aN_{\mathrm{VELO}} + b} \ , \tag{12}$$

where a and b are parameters that vary freely in the fit. Results of fits using Eq. 12 to determine the parametrization of the background scaling between the correlation functions for OS and SS pairs give $a = 0.044 \pm 0.004$ (0.075 ± 0.007) and $b = 1.86 \pm 0.12$ (3.12 ± 0.27) for pPb (Pbp).

6 Systematic uncertainties

Several sources of the systematic uncertainties are studied. The values determined for each of the sources are summarized in Table 3, where each input is assessed by taking the difference between the refitted correlation parameters and the baseline results, excluding the sources that proved to be negligible. The general approach to determine the systematic uncertainty is to repeat the analysis procedure with appropriate modifications introduced to evaluate the contribution in question. Some N_{VELO} bins display an outlying uncertainty of the correlation parameters, which is not representative of the other N_{VELO} regions, nevertheless they are shown in the final results.

The leading source of systematic uncertainty is due to the parametrization of non-femtoscopic background in the correlation function. It contains the effect related to the removal of the structures induced by two-body resonance decays from the fits to the OS correlation function. The impact of the particular choice of those limits is investigated by repeating the analysis with the widths of the defined regions increased and decreased by 20%. This value was already optimized in similar analyses performed by other experiments (*e.g.* Ref. [59]). Another effect in the determination of the cluster contribution is related to the choice of the range of the correlation function fits to the OS data, which is studied by varying its values within 10%, leading to the similar range variation as for the SS fit.

The impact of the N_0 value on the final correlation parameters is investigated by varying this value within $\sim$30%, i.e. from 10 to 20. The chosen value represents a conservative approach, as the systematic uncertainty related to N_0 value is minor with respect to other sources. The scaling of the cluster contribution amplitude between the OS and SS pairs is found to be the dominant contribution to the systematic uncertainty, reaching up to 9% (11%) for the R (λ) parameter. This was investigated by shifting the nominal parametrizations of the background scaling (see Eq. 11) determined for the central results by ± 0.15 before using them in the final SS fits to investigate the influence of this procedure on the measured correlation parameters. Those values are chosen to comprise most of the individual results with the z parameter left free in fits to the SS correlation function.

Table 3: Systematic uncertainties on the R and λ parameters. The listed ranges correspond to the lowest and highest values of the given input determined across most of the N_{VELO} bins in the pPb and Pbp samples (see the description in text for details). Negligible contributions are not listed. The total uncertainty is a quadratic sum of the individual inputs.

| | pPb dataset | | Pbp dataset | |
Contribution	$\sigma_{\mathrm{syst}}(R)$ [%]	$\sigma_{\mathrm{syst}}(\lambda)$ [%]	$\sigma_{\mathrm{syst}}(R)$ [%]	$\sigma_{\mathrm{syst}}(\lambda)$ [%]
Background scaling	4.5–9.0	3.5–11.0	4.5–6.5	3.0–9.5
Background fit range	1.0–3.0	0.5–3.5	2.0–3.5	0.5–4.0
Background fit – fixed N_0	0.5–3.0	0.5–3.0	< 0.5	< 0.5
Background fit – resonances	0.5–4.0	0.5–4.0	1.5–3.0	0.5–3.5
PID optimisation	0.5–1.5	0.5–5.0	0.5–10.5	0.5–8.5
Fake tracks	0.5–5.5	1.0–8.0	0.5–4.5	0.5–8.0
Requirement on z_{PV}	0.5–1.5	0.5–3.0	0.5–2.0	0.5–3.5
Coulomb correction	0.5–1.5	1.0–2.5	0.5–2.0	0.5–3.0
SS fit range (min)	1.5–5.0	1.0–8.5	0.5–3.5	0.5–5.5
SS fit range (max)	0.5–1.0	0.5–2.0	0.5–2.0	0.5–3.0
Reference sample	0.5–2.0	0.5–3.0	0.5–2.0	0.5–4.0
Total	6.0–12.0	6.0–16.5	6.5–12.0	5.0–16.0

Table 4: Fractions of fake tracks in the selected pion sample and in the signal pairs (with Q values restricted to the $Q < 1.0\,\mathrm{GeV}$ region) containing a fake track in the pPb and Pbp datasets. The values are determined using the simulation.

| | Single particle [%] | | Particle pair [%] | |
Probability to be a fake track	pPb	Pbp	pPb	Pbp
< 0.25	0.51	0.43	1.06	0.81
< 0.50	0.57	0.48	1.19	0.91

Systematic uncertainties related to the selection criteria involve the contribution related to the pion identification, which is based on the ProbNN(π) variable, by changing the requirement to increase the misidentified pions in the sample by $\sim$50% with respect to the final selection. Another contribution is related to the misreconstructed tracks, which may degrade the purity of the selected pion sample and affect the final results. The misreconstructed tracks (mostly the clone ones) that could directly contribute to the SS pairs in the BEC-signal region are well controlled in the data (see Sec. 4), so no uncertainty is assigned to the clone tracks. A dedicated study is performed to evaluate the impact of additional fake tracks in the sample by modifying the selection requirement on the probability for a particle to be a fake track from 0.25 to 0.50 (which corresponds to the maximum value available in the dataset after the preselection). The fractions of fake tracks in the selected pion sample and of signal pairs containing a fake track (values determined using the simulation) for those two criteria are $\leq$1% (see Table 4).

The contributions of the fake tracks and the pion selection criteria optimization to the systematic uncertainty are calculated as the absolute difference between the results obtained with the modified selection requirements and the central ones. In a limited

number of bins, those inputs constitute the most important contributions to the total systematic uncertainty, together with the one related to the background scaling.

Final-state Coulomb interactions for both the SS and OS pairs are taken into account in the fits to correlation functions. A simple proportionality $R_{\text{eff}} = \epsilon R$ is assumed [59] and the ϵ values are varied between 0.5 and 2.0. This leads to the final values of R_{eff} corresponding to 0.5 fm and 8.0 fm, which are used to evaluate the systematic uncertainty related to the correction for Coulomb interactions.

The range and binning used in the fit to the correlation functions for SS pairs can affect the final results. The impact from the boundary in the low-Q region is evaluated by altering it within 20%, which corresponds to the values of 0.04 and 0.06 GeV. A similar procedure is implemented for the fit boundary at high-Q values, where the modification at the level of 10% is applied, leading to the upper fit range being limited to 1.8 and extended to 2.2 GeV. The smaller relative variation in the case of the upper fit range is motivated to stay within the range where the used parametrization describes correctly the effect related to the long-range correlations. Both contributions to the systematic uncertainty associated with the SS fit range are found to be relatively small. The systematic uncertainty related to the binning of the Q variable in the correlation function is determined by doubling the bin width from the nominal 0.005 GeV to 0.010 GeV. The impact of this modification on the measured correlation parameters is negligible.

The construction of the reference sample is one of the basic aspects of the BEC analyses. The potential impact of the event-mixing implementation on the correlation parameters is assessed by varying the number of candidates available for the mixing, which is a parameter that can be tuned in the procedure. The nominal value of the number of candidates equal to 10 is changed to 50 and 100, and the analysis is repeated using the updated settings. The final contribution from the event-mixing to the systematic uncertainty is found to be small (see Table 3).

7 Results

The correlation parameters are determined by performing fits to the SS correlation functions in each individual N_{VELO} bin using Eq. 7. In this procedure, the parameters characterising the cluster contribution and the background scaling are fixed to the values measured in the previous steps of the analysis. The fits are performed in the full range of Q variable (0.05-2.00 GeV) in the constructed correlation functions. Example results of the final fits to the SS correlation functions are presented in Fig. 2. Correlation parameters determined from fits to the SS correlation functions using Eq. 7 in the N_{VELO} bins for the pPb and Pbp datasets are presented in Table 5. The fit quality in BEC studies is not expected to be ideal due to various assumptions in the signal parametrization and the unknown theoretical parameterization of the nonfemtoscopic background effects. The results are complementary to the measurements performed at LHC energies in central rapidity regions [55, 56, 59]. The measured behaviour of the correlation parameters is compatible with observations from other experiments at LHC. In general, the correlation radius becomes larger with increasing event multiplicity, while the intercept parameter displays the opposite behaviour. The determined R (λ) parameters vary within 1-4 fm ($\sim$0.40-0.85) depending on the N_{VELO} interval. Correlation parameters determined in the BEC studies for the pp [52], pPb and Pbp collisions at LHCb are illustrated in Figs. 3

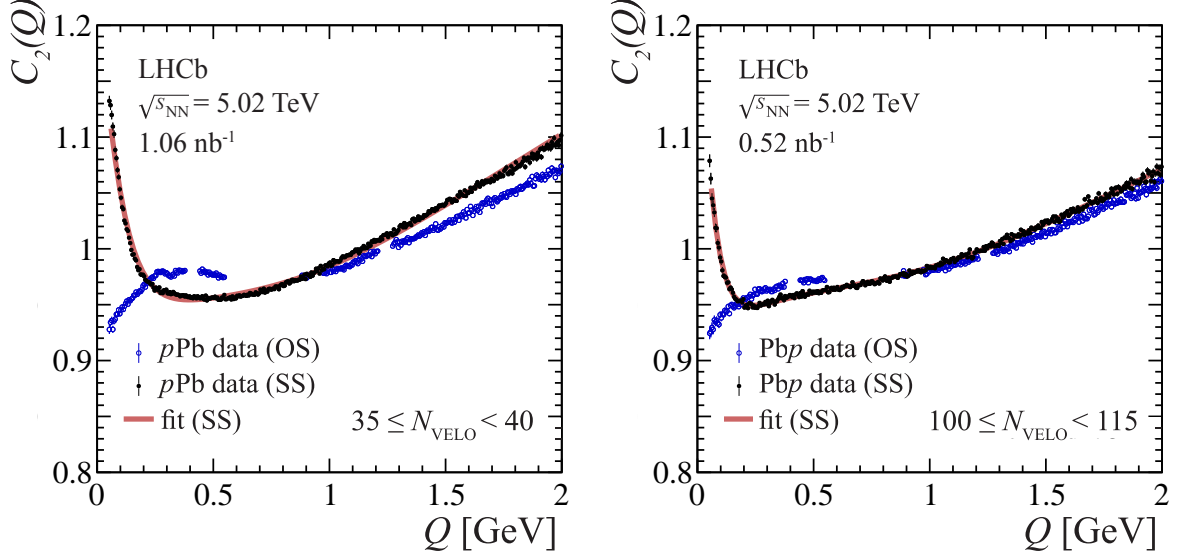Figure 2: Example of fits to the SS correlation functions in (left) a moderate-multiplicity region ($35 \leqslant N_{\mathrm{VELO}} < 40$) of the pPb and (right) high-multiplicity regime ($100 \leqslant N_{\mathrm{VELO}} < 115$) of the Pb$p$ dataset. The black points correspond to the SS correlation functions, while the blue ones illustrate the OS correlation functions which are used to estimate the cluster contribution in the given N_{VELO} bin. The results of fits using Eq. 7 are indicated by red solid lines. Only statistical uncertainties are shown.

and 4. As it is observed in Fig. 3 the measured correlation radii scale linearly with the cube root of the reconstructed charged-particle multiplicity. A simple fit illustrating this relationship is performed for different datasets (pp, pPb and Pbp). Only the statistical uncertainties of the measured R values are taken into account in this fit. Similar scaling was also reported by other experiments at LHC for various collision systems [46, 55, 59]. It is a tendency compatible with predictions of hydrodynamic models on the system evolution [91–94]. Although the results in both pPb and Pbp samples agree well within the systematic uncertainties, it may be observed that the central R values in the Pbp sample tend to be systematically higher than in the pPb case, becoming more prominent with increasing multiplicity.

Table 5: Correlation parameters determined from fits to the SS correlation functions using Eq. 7 in the N_{VELO} bins for the pPb and Pbp datasets. The first and second uncertainties are statistical and systematic, respectively.

	pPb dataset		Pbp dataset	
N_{VELO}	R [fm]	λ	R [fm]	λ
5–9	$1.159 \pm 0.010 \pm 0.070$	$0.860 \pm 0.006 \pm 0.056$	$1.227 \pm 0.013 \pm 0.080$	$0.791 \pm 0.007 \pm 0.045$
10–14	$1.413 \pm 0.010 \pm 0.105$	$0.635 \pm 0.004 \pm 0.037$	$1.469 \pm 0.013 \pm 0.108$	$0.630 \pm 0.005 \pm 0.031$
15–19	$1.638 \pm 0.011 \pm 0.131$	$0.562 \pm 0.004 \pm 0.033$	$1.658 \pm 0.014 \pm 0.135$	$0.548 \pm 0.005 \pm 0.036$
20–24	$1.790 \pm 0.011 \pm 0.161$	$0.516 \pm 0.004 \pm 0.036$	$1.801 \pm 0.015 \pm 0.148$	$0.487 \pm 0.005 \pm 0.038$
25–29	$1.944 \pm 0.012 \pm 0.189$	$0.476 \pm 0.004 \pm 0.039$	$1.989 \pm 0.017 \pm 0.150$	$0.467 \pm 0.005 \pm 0.036$
30–34	$2.088 \pm 0.014 \pm 0.214$	$0.464 \pm 0.004 \pm 0.044$	$2.130 \pm 0.019 \pm 0.169$	$0.444 \pm 0.005 \pm 0.037$
35–39	$2.218 \pm 0.016 \pm 0.225$	$0.452 \pm 0.005 \pm 0.044$	$2.279 \pm 0.021 \pm 0.206$	$0.433 \pm 0.006 \pm 0.045$
40–44	$2.364 \pm 0.019 \pm 0.250$	$0.443 \pm 0.005 \pm 0.049$	$2.380 \pm 0.024 \pm 0.233$	$0.409 \pm 0.006 \pm 0.051$
45–49	$2.482 \pm 0.023 \pm 0.271$	$0.435 \pm 0.006 \pm 0.052$	$2.554 \pm 0.027 \pm 0.220$	$0.415 \pm 0.007 \pm 0.047$
50–54	$2.575 \pm 0.028 \pm 0.281$	$0.427 \pm 0.008 \pm 0.053$	$2.725 \pm 0.031 \pm 0.259$	$0.416 \pm 0.008 \pm 0.048$
55–59	$2.730 \pm 0.036 \pm 0.322$	$0.443 \pm 0.010 \pm 0.070$	$2.875 \pm 0.035 \pm 0.252$	$0.420 \pm 0.009 \pm 0.046$
60–64	$2.799 \pm 0.046 \pm 0.341$	$0.427 \pm 0.012 \pm 0.070$	$2.972 \pm 0.040 \pm 0.306$	$0.412 \pm 0.010 \pm 0.062$
65–79	$2.972 \pm 0.045 \pm 0.318$	$0.415 \pm 0.011 \pm 0.059$	$3.322 \pm 0.028 \pm 0.324$	$0.448 \pm 0.007 \pm 0.062$
80–89	$3.462 \pm 0.115 \pm 0.410$	$0.479 \pm 0.033 \pm 0.118$	$3.531 \pm 0.043 \pm 0.337$	$0.449 \pm 0.011 \pm 0.070$
90–99	$3.535 \pm 0.219 \pm 0.635$	$0.485 \pm 0.062 \pm 0.196$	$3.871 \pm 0.052 \pm 0.320$	$0.513 \pm 0.015 \pm 0.081$
100–114	–	–	$3.854 \pm 0.049 \pm 0.270$	$0.513 \pm 0.015 \pm 0.072$
115–139	–	–	$3.863 \pm 0.049 \pm 0.468$	$0.555 \pm 0.016 \pm 0.057$
140–179	–	–	$3.225 \pm 0.053 \pm 0.979$	$0.487 \pm 0.016 \pm 0.096$

8 Conclusions

Bose-Einstein correlations in pairs of same-sign charged pions in pPb and Pbp collisions at LHCb are measured using a data-driven analysis method to account for effects related to the nonfemtoscopic background. The correlation parameters are determined in common intervals of VELO-track multiplicity. This measurement is the first of this type performed in the forward rapidity region at LHC energies. The correlation radius (the intercept parameter) increases (decreases) with the charged-particle multiplicity. This trend is consistent with observations in the central rapidity region by other experiments at the LHC [56, 59, 60]. The measured correlation radii scale linearly with the cube root of the charged-particle multiplicity, which is compatible with predictions based on hydrodynamic models [91, 92].
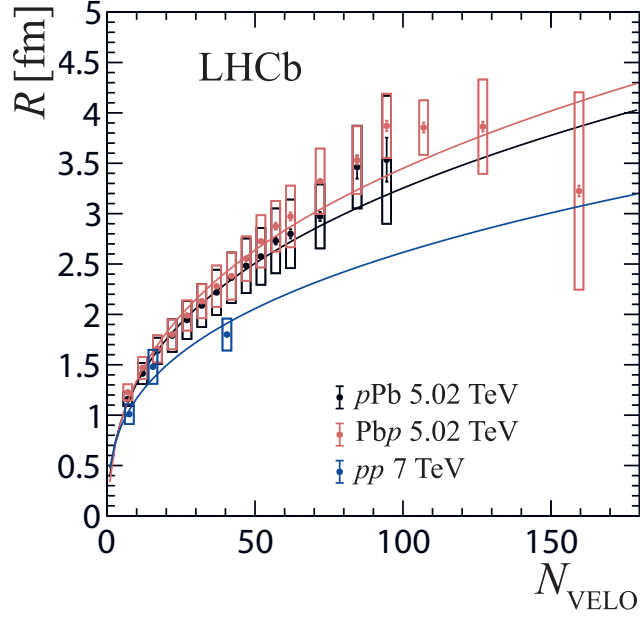
Figure 3: Correlation radius as a function of the reconstructed charged-particle multiplicity measured in the pp [52], pPb and Pbp collision systems in the LHCb experiment. Error bars indicate the statistical uncertainties, while boxes illustrate the systematic ones. Data points are positioned at the centres of the multiplicity bins. Results of the fits to the observed radii scale linearly in the cube root of the reconstructed multiplicity (solid lines).
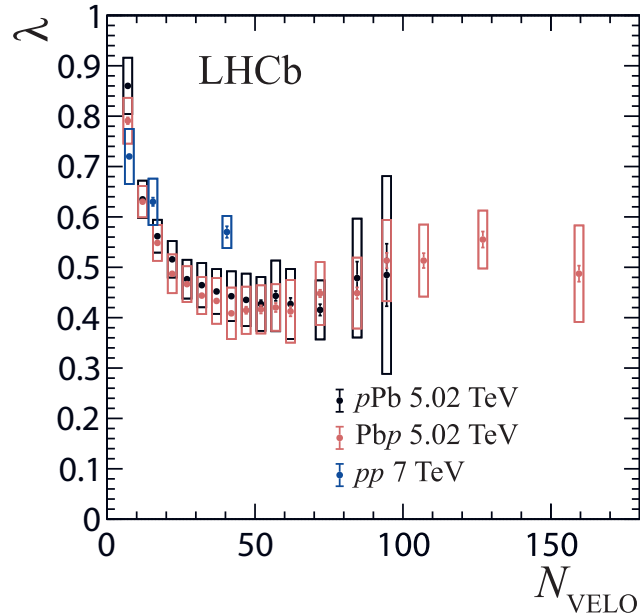

Figure 4: Intercept parameter as a function of the reconstructed charged-particle multiplicity measured in the pp [52], pPb and Pbp collision systems in the LHCb experiment. Error bars indicate the statistical uncertainties, while boxes illustrate the systematic ones. Data points are positioned at the centres of the multiplicity bins.

A Appendix. Distributions of the VELO-track multiplicity

The data samples are divided into bins of the VELO-track multiplicity, which is used as a proxy for the total charged-particle multiplicity. The division is optimized to obtain a high number of bins with enough entries to perform the measurement. This procedure is based on the N_{VELO} distribution for the signal pairs, which is shown in Fig. 5 and allows selecting bins with similar signal yields for the final analysis.
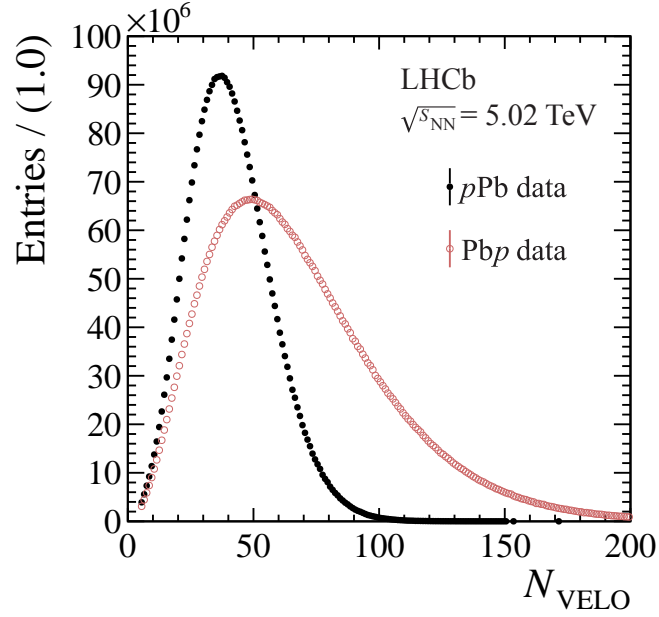

Figure 5: Distribution of the selected signal pairs originating from primary vertices with the given VELO-track multiplicity in the pPb (black dots) and Pbp (red circles) data.

Acknowledgements

References

[1] R. Hanbury Brown and R. Q. Twiss, *A New type of interferometer for use in radio astronomy*, Phil. Mag. Ser. 7 **45** (1954) 663.

[2] R. Hanbury Brown and R. Q. Twiss, *Correlation between photons in two coherent beams of light*, Nature **177** (1956) 27.

[3] R. Hanbury Brown and R. Q. Twiss, *A Test of a new type of stellar interferometer on Sirius*, Nature **178** (1956) 1046.

[4] A. N. Makhlin and Y. M. Sinyukov, *Hydrodynamics of hadron matter under pion interferometric microscope*, Z. Phys. **C39** (1988) 69.

[5] Y. M. Sinyukov, *Spectra and correlations in locally equilibrium hadron and quark - gluon systems*, Nucl. Phys. **A566** (1994) 589C.

[6] G. Goldhaber, W. B. Fowler, S. Goldhaber, and T. F. Hoang, *Pion-pion correlations in antiproton annihilation events*, Phys. Rev. Lett. **3** (1959) 181.

[7] W. A. Zajc *et al.*, *Two-pion correlations in heavy ion collisions*, Phys. Rev. **C29** (1984) 2173.

[8] E802 collaboration, L. Ahle *et al.*, *System, centrality, and transverse mass dependence of two pion correlation radii in heavy ion collisions at 11.6-A-GeV and 14.6-A-GeV*, Phys. Rev. **C66** (2002) 054906, `arXiv:nucl-ex/0204001`.

[9] Axial Field Spectrometer collaboration, T. Akesson *et al.*, *Bose-Einstein correlations in $\alpha\alpha$, pp and p$\bar{p}$ interactions*, Phys. Lett. **B129** (1983) 269.

[10] Axial Field Spectrometer collaboration, T. Akesson *et al.*, *Bose–Einstein correlations between kaons*, Phys. Lett. **B155** (1985) 128.

[11] Axial Field Spectrometer collaboration, T. Akesson *et al.*, *Evidence for a directional dependence of Bose-Einstein correlations at the CERN intersecting storage rings*, Phys. Lett. **B187** (1987) 420.

[12] UA1 collaboration, C. Albajar *et al.*, *Bose-Einstein correlations in $\bar{p}p$ interactions at $\sqrt{s}$ = 0.2 to 0.9 TeV*, Phys. Lett. **B226** (1989) 410, [Erratum: Phys.Lett.B 229, 439 (1989)].

[13] NA44 collaboration, H. Bøggild *et al.*, *Directional dependence of the pion source in high-energy heavy ion collisions*, Phys. Lett. **B349** (1995) 386.

[14] CERES collaboration, D. Adamová *et al.*, *Beam energy and centrality dependence of two pion Bose-Einstein correlations at SPS energies*, Nucl. Phys. **A714** (2003) 124, `arXiv:nucl-ex/0207005`.

[15] ALEPH collaboration, D. Decamp *et al.*, *A study of Bose-Einstein correlations in e^+e^- annihilation at 91 GeV*, Z. Phys. **C54** (1992) 75.

[16] ALEPH collaboration, D. Buskulic *et al.*, *Production of K^0 and Λ in hadronic Z decays*, Z. Phys. **C64** (1994) 361.

[17] ALEPH collaboration, R. Barate *et al.*, *Fermi-Dirac correlations in Λ pairs in hadronic Z decays*, Phys. Lett. **B475** (2000) 395.

[18] ALEPH collaboration, A. Heister *et al.*, *Two-dimensional analysis of Bose-Einstein correlations in hadronic Z decays at LEP*, Eur. Phys. J. **C36** (2004) 147.

[19] DELPHI collaboration, P. Abreu *et al.*, *Bose-Einstein correlations in the hadronic decays of the Z^0*, Phys. Lett. **B286** (1992) 201.

[20] DELPHI collaboration, P. Abreu *et al.*, *Kaon interference in the hadronic decays of the Z^0*, Phys. Lett. **B379** (1996) 330.

[21] DELPHI collaboration, P. Abreu *et al.*, *Two-dimensional analysis of the Bose-Einstein correlations in e^+e^- annihilation at the Z^0 peak*, Phys. Lett. **B471** (2000) 460.

[22] L3 collaboration, M. Acciarri *et al.*, *Measurement of an elongation of the pion source in Z decays*, Phys. Lett. **B458** (1999) 517, `arXiv:hep-ex/9909009`.

[23] L3 collaboration, P. Achard *et al.*, *Bose-Einstein correlations of neutral and charged pions in hadronic Z decays*, Phys. Lett. **B524** (2002) 55, `arXiv:hep-ex/0109036`.

[24] L3 collaboration, P. Achard *et al.*, *Test of the τ-model of Bose-Einstein correlations and reconstruction of the source function in hadronic Z-boson decay at LEP*, Eur. Phys. J. **C71** (2011) 1648, `arXiv:1105.4788`.

[25] OPAL collaboration, G. Abbiendi *et al.*, *Bose-Einstein correlations in $K^{\pm}K^{\pm}$ pairs from Z decays into two hadronic jets*, Eur. Phys. J. **C21** (2001) 23, `arXiv:hep-ex/0001045`.

[26] OPAL collaboration, R. Akers *et al.*, *The production of neutral kaons in Z^0 decays and their Bose-Einstein correlations*, Z. Phys. **C67** (1995) 389.

[27] OPAL collaboration, G. Alexander *et al.*, *A First measurement of the $\Lambda\bar{\Lambda}$ and $\Lambda\Lambda$ ($\bar{\Lambda}\bar{\Lambda}$) spin compositions in hadronic Z^0 decays*, Phys. Lett. **B384** (1996) 377.

[28] OPAL collaboration, G. Alexander *et al.*, *Multiplicity dependence of Bose-Einstein correlations in hadronic Z^0 decays*, Z. Phys. **C72** (1996) 389.

[29] OPAL collaboration, G. Abbiendi *et al.*, *Transverse and longitudinal Bose Einstein correlations in hadronic Z^0 decays*, Eur. Phys. J. **C16** (2000) 423, `arXiv:hep-ex/0002062`.

[30] OPAL collaboration, G. Abbiendi *et al.*, *Bose-Einstein correlations of π^0 pairs from hadronic Z decays*, Phys. Lett. **B559** (2003) 131, `arXiv:hep-ex/0302027`.

[31] STAR collaboration, C. Adler *et al.*, *Pion interferometry of $\sqrt{s_{NN}} = 130\,GeV$ $Au+Au$ collisions at RHIC*, Phys. Rev. Lett. **87** (2001) 082301, `arXiv:nucl-ex/0107008`.

[32] STAR collaboration, J. Adams *et al.*, *Three pion HBT correlations in relativistic heavy ion collisions from the STAR experiment*, Phys. Rev. Lett. **91** (2003) 262301, `arXiv:nucl-ex/0306028`.

[33] STAR collaboration, J. Adams *et al.*, *Azimuthally sensitive HBT in Au+Au collisions at $\sqrt{s_{NN}} = 200\,GeV$*, Phys. Rev. Lett. **93** (2004) 012301, `arXiv:nucl-ex/0312009`.

[34] STAR collaboration, J. Adams *et al.*, *Pion interferometry in Au+Au collisions at $\sqrt{s_{NN}} = 200\,GeV$*, Phys. Rev. **C71** (2005) 044906, `arXiv:nucl-ex/0411036`.

[35] STAR collaboration, B. I. Abelev *et al.*, *Pion Interferometry in Au+Au and Cu+Cu Collisions at RHIC*, Phys. Rev. **C80** (2009) 024905, `arXiv:0903.1296`.

[36] STAR collaboration, L. Adamczyk *et al.*, *Freeze-out dynamics via charged kaon femtoscopy in $\sqrt{s_{NN}} = 200\ GeV$ central Au+Au collisions*, Phys. Rev. **C88** (2013) 034906, `arXiv:1302.3168`.

[37] STAR collaboration, L. Adamczyk *et al.*, *Beam-energy-dependent two-pion interferometry and the freeze-out eccentricity of pions measured in heavy ion collisions at the STAR detector*, Phys. Rev. **C92** (2015) 014904, `arXiv:1403.4972`.

[38] PHENIX collaboration, S. S. Adler *et al.*, *Bose-Einstein correlations of charged pion pairs in Au+Au collisions at $\sqrt{s_{NN}} = 200\,GeV$*, Phys. Rev. Lett. **93** (2004) 152302, `arXiv:nucl-ex/0401003`.

[39] STAR collaboration, M. M. Aggarwal *et al.*, *Pion femtoscopy in p+p collisions at $\sqrt{s}$=200 GeV*, Phys. Rev. **C83** (2011) 064905, `arXiv:1004.0925`.

[40] PHENIX collaboration, S. Afanasiev *et al.*, *Source breakup dynamics in Au+Au Collisions at $\sqrt{s_{NN}} = 200\,GeV$ via three-dimensional two-pion source imaging*, Phys. Rev. Lett. **100** (2008) 232301, `arXiv:0712.4372`.

[41] PHENIX collaboration, A. Adare *et al.*, *Energy Loss and Flow of Heavy Quarks in Au+Au Collisions at $\sqrt{s_{NN}} = 200\,GeV$*, Phys. Rev. Lett. **98** (2007) 172301, `arXiv:nucl-ex/0611018`.

[42] PHENIX collaboration, A. Adare *et al.*, *Lévy-stable two-pion Bose-Einstein correlations in $\sqrt{s_{NN}}$=200 GeV Au+Au collisions*, Phys. Rev. **C97** (2018) 064911, `arXiv:1709.05649`.

[43] PHOBOS collaboration, B. B. Back *et al.*, *Transverse momentum and rapidity dependence of HBT correlations in Au+Au collisions at $\sqrt{s_{NN}} = 62.4\,GeV$ and $200\,GeV$*, Phys. Rev. **C73** (2006) 031901, `arXiv:nucl-ex/0409001`.

[44] CMS collaboration, V. Khachatryan *et al.*, *First measurement of Bose-Einstein correlations in proton-proton collisions at $\sqrt{s}$ =0.9 and 2.36 TeV at the LHC*, Phys. Rev. Lett. **105** (2010) 032001, `arXiv:1005.3294`.

[45] CMS collaboration, V. Khachatryan *et al.*, *Measurement of Bose-Einstein correlations in pp collisions at $\sqrt{s}$=0.9 and 7 TeV*, JHEP **05** (2011) 029, `arXiv:1101.3518`.

[46] CMS collaboration, A. M. Sirunyan *et al.*, *Bose-Einstein correlations of charged hadrons in proton-proton collisions at $\sqrt{s} = 13$ TeV*, JHEP **03** (2020) 014, `arXiv:1910.08815`.

[47] ALICE collaboration, K. Aamodt *et al.*, *Two-pion Bose-Einstein correlations in pp collisions at $\sqrt{s} = 900$ GeV*, Phys. Rev. **D82** (2010) 052001, `arXiv:1007.0516`.

[48] ALICE collaboration, B. Abelev *et al.*, *K_S^0-K_S^0 correlations in pp collisions at $\sqrt{s} = 7$ TeV from the LHC ALICE experiment*, Phys. Lett. **B717** (2012) 151, `arXiv:1206.2056`.

[49] ALICE collaboration, B. Abelev *et al.*, *Charged kaon femtoscopic correlations in pp collisions at $\sqrt{s} = 7$ TeV*, Phys. Rev. **D87** (2013) 052016, `arXiv:1212.5958`.

[50] ALICE collaboration, S. Acharya *et al.*, *p-p, p-Λ and Λ-Λ correlations studied via femtoscopy in pp reactions at $\sqrt{s} = 7$ TeV*, Phys. Rev. **C99** (2019) 024001, `arXiv:1805.12455`.

[51] ATLAS collaboration, G. Aad *et al.*, *Two-particle Bose–Einstein correlations in pp collisions at $\sqrt{s} = 0.9$ and 7 TeV measured with the ATLAS detector*, Eur. Phys. J. **C75** (2015) 466, `arXiv:1502.07947`.

[52] LHCb collaboration, R. Aaij *et al.*, *Bose–Einstein correlations of same-sign charged pions in the forward region in pp collisions at $\sqrt{s} = 7$ TeV*, JHEP **12** (2017) 025, `arXiv:1709.01769`.

[53] ALICE collaboration, K. Aamodt *et al.*, *Femtoscopy of pp collisions at $\sqrt{s} = 0.9$ and 7 TeV at the LHC with two-pion Bose-Einstein correlations*, Phys. Rev. **D84** (2011) 112004, `arXiv:1101.3665`.

[54] ALICE collaboration, B. Abelev *et al.*, *Freeze-out radii extracted from three-pion cumulants in pp, p–Pb and Pb–Pb collisions at the LHC*, Phys. Lett. **B739** (2014) 139, `arXiv:1404.1194`.

[55] ALICE collaboration, J. Adam *et al.*, *Multipion Bose-Einstein correlations in pp,p-Pb, and Pb-Pb collisions at energies available at the CERN Large Hadron Collider*, Phys. Rev. **C93** (2016) 054908, `arXiv:1512.08902`.

[56] CMS collaboration, A. M. Sirunyan *et al.*, *Bose-Einstein correlations in pp, pPb, and PbPb collisions at $\sqrt{s_{NN}} = 0.9$-7 TeV*, Phys. Rev. **C97** (2018) 064912, `arXiv:1712.07198`.

[57] ALICE collaboration, S. Acharya *et al.*, *Study of the Λ-Λ interaction with femtoscopy correlations in pp and p-Pb collisions at the LHC*, Phys. Lett. **B797** (2019) 134822, `arXiv:1905.07209`.

[58] ALICE collaboration, S. Acharya *et al.*, *One-dimensional charged kaon femtoscopy in p-Pb collisions at $\sqrt{s_{NN}} = 5.02$ TeV*, Phys. Rev. **C100** (2019) 024002, `arXiv:1903.12310`.

[59] ATLAS collaboration, M. Aaboud *et al.*, *Femtoscopy with identified charged pions in proton-lead collisions at $\sqrt{s_{NN}}$ =5.02 TeV with ATLAS*, Phys. Rev. **C96** (2017) 064908, `arXiv:1704.01621`.

[60] ALICE collaboration, J. Adam *et al.*, *Two-pion femtoscopy in p-Pb collisions at $\sqrt{s_{NN}}$ =5.02 TeV*, Phys. Rev. **C91** (2015) 034906, `arXiv:1502.00559`.

[61] ALICE collaboration, S. Acharya *et al.*, *Kaon femtoscopy in Pb-Pb collisions at $\sqrt{s_{NN}}$ = 2.76 TeV*, Phys. Rev. **C96** (2017) 064613, `arXiv:1709.01731`.

[62] ALICE collaboration, K. Aamodt *et al.*, *Two-pion Bose-Einstein correlations in central Pb-Pb collisions at $\sqrt{s_{NN}}$ = 2.76 TeV*, Phys. Lett. **B696** (2011) 328, `arXiv:1012.4035`.

[63] T. Alexopoulos *et al.*, *A Study of source size in $p\overline{p}$ collisions at $\sqrt{s}$ = 1.8 TeV using pion interferometry*, Phys. Rev. **D48** (1993) 1931.

[64] H1 collaboration, C. Adloff *et al.*, *Bose-Einstein correlations in deep inelastic ep scattering at HERA*, Z. Phys. **C75** (1997) 437, `arXiv:hep-ex/9705001`.

[65] T. Csorgo, *Particle interferometry from 40 MeV to 40 TeV*, Acta Phys. Hung. **A15** (2002) 1, `arXiv:hep-ph/0001233`.

[66] W. Kittel, *Bose-Einstein correlations in Z fragmentation and other reactions*, Acta Phys. Polon. **B32** (2001) 3927, `arXiv:hep-ph/0110088`.

[67] G. Baym, *The physics of Hanbury Brown–Twiss intensity interferometry: from stars to nuclear collisions*, Acta Phys. Polon. **B29** (1998) 1839, `arXiv:nucl-th/9804026`.

[68] T. Csorgo, S. Hegyi, and W. A. Zajc, *Bose–Einstein correlations for Lévy stable source distributions*, Eur. Phys. J. **C36** (2004) 67, `arXiv:nucl-th/0310042`.

[69] M. G. Bowler, *Coulomb corrections to Bose–Einstein correlations have been greatly exaggerated*, Phys. Lett. **B270** (1991) 69.

[70] Y. Sinyukov *et al.*, *Coulomb corrections for interferometry analysis of expanding hadron systems*, Phys. Lett. **B432** (1998) 248.

[71] M. Csanád, S. Lökös, and M. Nagy, *Coulomb final state interaction in heavy ion collisions for Lévy sources*, Universe **5** (2019) 133, `arXiv:1905.09714`.

[72] S. Pratt, *Coherence and Coulomb effects on pion interferometry*, Phys. Rev. **D33** (1986) 72.

[73] W. Kittel, *Bose-Einstein correlations in Z fragmentation and other reactions*, Acta Phys. Polon. **B32** (2001) 3927, `arXiv:hep-ph/0110088`.

[74] G. Alexander, *Bose–Einstein and Fermi–Dirac interferometry in particle physics*, Rept. Prog. Phys. **66** (2003) 481, `arXiv:hep-ph/0302130`.

[75] T. Csorgo, B. Lorstad, and J. Zimanyi, *Bose-Einstein correlations for systems with large halo*, Z. Phys. C **71** (1996) 491, `arXiv:hep-ph/9411307`.

[76] LHCb collaboration, A. A. Alves Jr. *et al.*, *The LHCb detector at the LHC*, JINST **3** (2008) S08005.

[77] LHCb collaboration, R. Aaij *et al.*, *LHCb detector performance*, Int. J. Mod. Phys. **A30** (2015) 1530022, arXiv:1412.6352.

[78] R. Aaij *et al.*, *Performance of the LHCb Vertex Locator*, JINST **9** (2014) P09007, arXiv:1405.7808.

[79] R. Arink *et al.*, *Performance of the LHCb Outer Tracker*, JINST **9** (2014) P01002, arXiv:1311.3893.

[80] M. Adinolfi *et al.*, *Performance of the LHCb RICH detector at the LHC*, Eur. Phys. J. **C73** (2013) 2431, arXiv:1211.6759.

[81] A. A. Alves Jr. *et al.*, *Performance of the LHCb muon system*, JINST **8** (2013) P02022, arXiv:1211.1346.

[82] R. Aaij *et al.*, *The LHCb trigger and its performance in 2011*, JINST **8** (2013) P04022, arXiv:1211.3055.

[83] T. Pierog *et al.*, *EPOS LHC: Test of collective hadronization with data measured at the CERN Large Hadron Collider*, Phys. Rev. **C92** (2015) 034906, arXiv:1306.0121.

[84] I. Belyaev *et al.*, *Handling of the generation of primary events in Gauss, the LHCb simulation framework*, J. Phys. Conf. Ser. **331** (2011) 032047.

[85] D. J. Lange, *The EvtGen particle decay simulation package*, Nucl. Instrum. Meth. **A462** (2001) 152.

[86] P. Golonka and Z. Was, *PHOTOS Monte Carlo: A precision tool for QED corrections in Z and W decays*, Eur. Phys. J. **C45** (2006) 97.

[87] Geant4 collaboration, J. Allison *et al.*, *Geant4 developments and applications*, IEEE Trans. Nucl. Sci. **53** (2006) 270.

[88] Geant4 collaboration, S. Agostinelli *et al.*, *Geant4: A simulation toolkit*, Nucl. Instrum. Meth. **A506** (2003) 250.

[89] M. Clemencic *et al.*, *The LHCb simulation application, Gauss: Design, evolution and experience*, J. Phys. Conf. Ser. **331** (2011) 032023.

[90] L. Anderlini *et al.*, *The PIDCalib package*, LHCb-PUB-2016-021, 2016.

[91] K. Werner *et al.*, *Evidence for hydrodynamic evolution in proton-proton scattering at 900 GeV*, Phys. Rev. **C83** (2011) 044915, arXiv:1010.0400.

[92] P. Bozek and W. Broniowski, *Size of the emission source and collectivity in ultra-relativistic p-Pb collisions*, Phys. Lett. **B720** (2013) 250, arXiv:1301.3314.

[93] V. M. Shapoval, P. Braun-Munzinger, I. A. Karpenko, and Y. M. Sinyukov, *Femto-scopic scales in p+p and p+Pb collisions in view of the uncertainty principle*, Phys. Lett. **B725** (2013) 139, arXiv:1304.3815.

[94] B. Schenke and R. Venugopalan, *Eccentric protons? Sensitivity of flow to system size and shape in p+p, p+Pb and Pb+Pb collisions*, Phys. Rev. Lett. **113** (2014) 102301, arXiv:1405.3605.

LHCb collaboration

R. Aaij[32] , A.S.W. Abdelmotteleb[51] , C. Abellan Beteta[45], F. Abudinén[51] ,
T. Ackernley[55] , B. Adeva[41] , M. Adinolfi[49] , P. Adlarson[77] , H. Afsharnia[9],
C. Agapopoulou[43] , C.A. Aidala[78] , Z. Ajaltouni[9], S. Akar[60] , K. Akiba[32] ,
P. Albicocco[23] , J. Albrecht[15] , F. Alessio[43] , M. Alexander[54] , A. Alfonso Albero[40] ,
Z. Aliouche[57] , P. Alvarez Cartelle[50] , R. Amalric[13] , S. Amato[2] , J.L. Amey[49] ,
Y. Amhis[11,43] , L. An[5] , L. Anderlini[22] , M. Andersson[45] , A. Andreianov[38] ,
M. Andreotti[21] , D. Andreou[63] , D. Ao[6] , F. Archilli[31,t] , A. Artamonov[38] ,
M. Artuso[63] , E. Aslanides[10] , M. Atzeni[45] , B. Audurier[12] , I.B Bachiller Perea[8] ,
S. Bachmann[17] , M. Bachmayer[44] , J.J. Back[51] , A. Bailly-reyre[13],
P. Baladron Rodriguez[41] , V. Balagura[12] , W. Baldini[21,43] , J. Baptista de Souza Leite[1] ,
M. Barbetti[22,j] , R.J. Barlow[57] , S. Barsuk[11] , W. Barter[53] , M. Bartolini[50] ,
F. Baryshnikov[38] , J.M. Basels[14] , G. Bassi[29,q] , B. Batsukh[4] , A. Battig[15] ,
A. Bay[44] , A. Beck[51] , M. Becker[15] , F. Bedeschi[29] , I.B. Bediaga[1] , A. Beiter[63],
S. Belin[41] , V. Bellee[45] , K. Belous[38] , I. Belov[38] , I. Belyaev[38] , G. Benane[10] ,
G. Bencivenni[23] , E. Ben-Haim[13] , A. Berezhnoy[38] , R. Bernet[45] , S. Bernet Andres[39] ,
D. Berninghoff[17], H.C. Bernstein[63], C. Bertella[57] , A. Bertolin[28] , C. Betancourt[45] ,
F. Betti[43] , Ia. Bezshyiko[45] , J. Bhom[35] , L. Bian[69] , M.S. Bieker[15] , N.V. Biesuz[21] ,
P. Billoir[13] , A. Biolchini[32] , M. Birch[56] , F.C.R. Bishop[50] , A. Bitadze[57] ,
A. Bizzeti , M.P. Blago[50] , T. Blake[51] , F. Blanc[44] , J.E. Blank[15] , S. Blusk[63] ,
D. Bobulska[54] , V.B Bocharnikov[38] , J.A. Boelhauve[15] , O. Boente Garcia[12] ,
T. Boettcher[60] , A. Boldyrev[38] , C.S. Bolognani[75] , R. Bolzonella[21,i] , N. Bondar[38] ,
F. Borgato[28] , S. Borghi[57] , M. Borsato[17] , J.T. Borsuk[35] , S.A. Bouchiba[44] ,
T.J.V. Bowcock[55] , A. Boyer[43] , C. Bozzi[21] , M.J. Bradley[56], S. Braun[61] ,
A. Brea Rodriguez[41] , N. Breer[15] , J. Brodzicka[35] , A. Brossa Gonzalo[41] , J. Brown[55] ,
D. Brundu[27] , A. Buonaura[45] , L. Buonincontri[28] , A.T. Burke[57] , C. Burr[43] ,
A. Bursche[67], A. Butkevich[38] , J.S. Butter[32] , J. Buytaert[43] , W. Byczynski[43] ,
S. Cadeddu[27] , H. Cai[69], R. Calabrese[21,i] , L. Calefice[15] , S. Cali[23] , M. Calvi[26,m] ,
M. Calvo Gomez[39] , P. Campana[23] , D.H. Campora Perez[75] ,
A.F. Campoverde Quezada[6] , S. Capelli[26,m] , L. Capriotti[21] , A. Carbone[20,g] ,
R. Cardinale[24,k] , A. Cardini[27] , P. Carniti[26,m] , L. Carus[14], A. Casais Vidal[41] ,
R. Caspary[17] , G. Casse[55] , M. Cattaneo[43] , G. Cavallero[21] , V. Cavallini[21,i] ,
S. Celani[44] , J. Cerasoli[10] , D. Cervenkov[58] , A.J. Chadwick[55] , I. Chahrour[78] ,
M.G. Chapman[49], M. Charles[13] , Ph. Charpentier[43] , C.A. Chavez Barajas[55] ,
M. Chefdeville[8] , C. Chen[10] , S. Chen[4] , A. Chernov[35] , S. Chernyshenko[47] ,
V. Chobanova[41,w] , S. Cholak[44] , M. Chrzaszcz[35] , A. Chubykin[38] , V. Chulikov[38] ,
P. Ciambrone[23] , M.F. Cicala[51] , X. Cid Vidal[41] , G. Ciezarek[43] , P. Cifra[43] ,
G. Ciullo[i,21] , P.E.L. Clarke[53] , M. Clemencic[43] , H.V. Cliff[50] , J. Closier[43] ,
J.L. Cobbledick[57] , V. Coco[43] , J. Cogan[10] , E. Cogneras[9] , L. Cojocariu[37] ,
P. Collins[43] , T. Colombo[43] , L. Congedo[19] , A. Contu[27] , N. Cooke[48] ,
I. Corredoira [41] , G. Corti[43] , B. Couturier[43] , D.C. Craik[45] , M. Cruz Torres[1,e] ,
R. Currie[53] , C.L. Da Silva[62] , S. Dadabaev[38] , L. Dai[66] , X. Dai[5] , E. Dall'Occo[15] ,
J. Dalseno[41] , C. D'Ambrosio[43] , J. Daniel[9] , A. Danilina[38] , P. d'Argent[19] ,
J.E. Davies[57] , A. Davis[57] , O. De Aguiar Francisco[57] , J. de Boer[43] , K. De Bruyn[74] ,
S. De Capua[57] , M. De Cian[44] , U. De Freitas Carneiro Da Graca[1] , E. De Lucia[23] ,
J.M. De Miranda[1] , L. De Paula[2] , M. De Serio[19,f] , D. De Simone[45] , P. De Simone[23] ,
F. De Vellis[15] , J.A. de Vries[75] , C.T. Dean[62] , F. Debernardis[19,f] , D. Decamp[8] ,
V. Dedu[10] , L. Del Buono[13] , B. Delaney[59] , H.-P. Dembinski[15] , V. Denysenko[45] ,
O. Deschamps[9] , F. Dettori[27,h] , B. Dey[72] , P. Di Nezza[23] , I. Diachkov[38] ,

S. Didenko[38] (iD), L. Dieste Maronas[41], S. Ding[63] (iD), V. Dobishuk[47] (iD), A. Dolmatov[38],
C. Dong[3] (iD), A.M. Donohoe[18] (iD), F. Dordei[27] (iD), A.C. dos Reis[1] (iD), L. Douglas[54],
A.G. Downes[8] (iD), P. Duda[76] (iD), M.W. Dudek[35] (iD), L. Dufour[43] (iD), V. Duk[73] (iD), P. Durante[43] (iD),
M. M. Duras[76] (iD), J.M. Durham[62] (iD), D. Dutta[57] (iD), A. Dziurda[35] (iD), A. Dzyuba[38] (iD),
S. Easo[52] (iD), U. Egede[64] (iD), A. Egorychev[38] (iD), V. Egorychev[38] (iD), C. Eirea Orro[41],
S. Eisenhardt[53] (iD), E. Ejopu[57] (iD), S. Ek-In[44] (iD), L. Eklund[77] (iD), M.E Elashri[60] (iD),
J. Ellbracht[15] (iD), S. Ely[56] (iD), A. Ene[37] (iD), E. Epple[60] (iD), S. Escher[14] (iD), J. Eschle[45] (iD),
S. Esen[45] (iD), T. Evans[57] (iD), F. Fabiano[27,h] (iD), L.N. Falcao[1] (iD), Y. Fan[6] (iD), B. Fang[11,69] (iD),
L. Fantini[73,p] (iD), M. Faria[44] (iD), S. Farry[55] (iD), D. Fazzini[26,m] (iD), L.F Felkowski[76] (iD), M. Feo[43] (iD),
M. Fernandez Gomez[41] (iD), A.D. Fernez[61] (iD), F. Ferrari[20] (iD), L. Ferreira Lopes[44] (iD),
F. Ferreira Rodrigues[2] (iD), S. Ferreres Sole[32] (iD), M. Ferrillo[45] (iD), M. Ferro-Luzzi[43] (iD),
S. Filippov[38] (iD), R.A. Fini[19] (iD), M. Fiorini[21,i] (iD), M. Firlej[34] (iD), K.M. Fischer[58] (iD),
D.S. Fitzgerald[78] (iD), C. Fitzpatrick[57] (iD), T. Fiutowski[34] (iD), F. Fleuret[12] (iD), M. Fontana[20] (iD),
F. Fontanelli[24,k] (iD), R. Forty[43] (iD), D. Foulds-Holt[50] (iD), V. Franco Lima[55] (iD),
M. Franco Sevilla[61] (iD), M. Frank[43] (iD), E. Franzoso[21,i] (iD), G. Frau[17] (iD), C. Frei[43] (iD),
D.A. Friday[57] (iD), L.F Frontini[25,l] (iD), J. Fu[6] (iD), Q. Fuehring[15] (iD), T. Fulghesu[13] (iD),
E. Gabriel[32] (iD), G. Galati[19,f] (iD), M.D. Galati[32] (iD), A. Gallas Torreira[41] (iD), D. Galli[20,g] (iD),
S. Gambetta[53,43] (iD), M. Gandelman[2] (iD), P. Gandini[25] (iD), H.G Gao[6] (iD), R. Gao[58] (iD), Y. Gao[7] (iD),
Y. Gao[5] (iD), M. Garau[27,h] (iD), L.M. Garcia Martin[51] (iD), P. Garcia Moreno[40] (iD),
J. García Pardiñas[43] (iD), B. Garcia Plana[41], F.A. Garcia Rosales[12] (iD), L. Garrido[40] (iD),
C. Gaspar[43] (iD), R.E. Geertsema[32] (iD), D. Gerick[17], L.L. Gerken[15] (iD), E. Gersabeck[57] (iD),
M. Gersabeck[57] (iD), T. Gershon[51] (iD), L. Giambastiani[28] (iD), V. Gibson[50] (iD), H.K. Giemza[36] (iD),
A.L. Gilman[58] (iD), M. Giovannetti[23] (iD), A. Gioventù[41] (iD), P. Gironella Gironell[40] (iD),
C. Giugliano[21,i] (iD), M.A. Giza[35] (iD), K. Gizdov[53] (iD), E.L. Gkougkousis[43] (iD), V.V. Gligorov[13] (iD),
C. Göbel[65] (iD), E. Golobardes[39] (iD), D. Golubkov[38] (iD), A. Golutvin[56,38] (iD), A. Gomes[1,a] (iD),
S. Gomez Fernandez[40] (iD), F. Goncalves Abrantes[58] (iD), M. Goncerz[35] (iD), G. Gong[3] (iD),
I.V. Gorelov[38] (iD), C. Gotti[26] (iD), J.P. Grabowski[71] (iD), T. Grammatico[13] (iD),
L.A. Granado Cardoso[43] (iD), E. Graugés[40] (iD), E. Graverini[44] (iD), G. Graziani (iD), A. T. Grecu[37] (iD),
L.M. Greeven[32] (iD), N.A. Grieser[60] (iD), L. Grillo[54] (iD), S. Gromov[38] (iD), C. Gu[3] (iD),
M. Guarise[21,i] (iD), M. Guittiere[11] (iD), V. Guliaeva[38] (iD), P. A. Günther[17] (iD), A.K. Guseinov[38] (iD),
E. Gushchin[38] (iD), Y. Guz[5,38,43] (iD), T. Gys[43] (iD), T. Hadavizadeh[64] (iD), C. Hadjivasiliou[61] (iD),
G. Haefeli[44] (iD), C. Haen[43] (iD), J. Haimberger[43] (iD), S.C. Haines[50] (iD), T. Halewood-leagas[55] (iD),
M.M. Halvorsen[43] (iD), P.M. Hamilton[61] (iD), J. Hammerich[55] (iD), Q. Han[7] (iD), X. Han[17] (iD),
S. Hansmann-Menzemer[17] (iD), L. Hao[6] (iD), N. Harnew[58] (iD), T. Harrison[55] (iD), C. Hasse[43] (iD),
M. Hatch[43] (iD), J. He[6,c] (iD), K. Heijhoff[32] (iD), F.H Hemmer[43] (iD), C. Henderson[60] (iD),
R.D.L. Henderson[64,51] (iD), A.M. Hennequin[59] (iD), K. Hennessy[55] (iD), L. Henry[43] (iD), J. Herd[56] (iD),
J. Heuel[14] (iD), A. Hicheur[2] (iD), D. Hill[44] (iD), M. Hilton[57] (iD), S.E. Hollitt[15] (iD), J. Horswill[57] (iD),
R. Hou[7] (iD), Y. Hou[8] (iD), J. Hu[17], J. Hu[67] (iD), W. Hu[5] (iD), X. Hu[3] (iD), W. Huang[6] (iD), X. Huang[69],
W. Hulsbergen[32] (iD), R.J. Hunter[51] (iD), M. Hushchyn[38] (iD), D. Hutchcroft[55] (iD), P. Ibis[15] (iD),
M. Idzik[34] (iD), D. Ilin[38] (iD), P. Ilten[60] (iD), A. Inglessi[38] (iD), A. Iniukhin[38] (iD), A. Ishteev[38] (iD),
K. Ivshin[38] (iD), R. Jacobsson[43] (iD), H. Jage[14] (iD), S.J. Jaimes Elles[42] (iD), S. Jakobsen[43] (iD),
E. Jans[32] (iD), B.K. Jashal[42] (iD), A. Jawahery[61] (iD), V. Jevtic[15] (iD), E. Jiang[61] (iD), X. Jiang[4,6] (iD),
Y. Jiang[6] (iD), M. John[58] (iD), D. Johnson[59] (iD), C.R. Jones[50] (iD), T.P. Jones[51] (iD), S.J Joshi[36] (iD),
B. Jost[43] (iD), N. Jurik[43] (iD), I. Juszczak[35] (iD), S. Kandybei[46] (iD), Y. Kang[3] (iD), M. Karacson[43] (iD),
D. Karpenkov[38] (iD), M. Karpov[38] (iD), J.W. Kautz[60] (iD), F. Keizer[43] (iD), D.M. Keller[63] (iD),
M. Kenzie[51] (iD), T. Ketel[32] (iD), B. Khanji[63] (iD), A. Kharisova[38] (iD), S. Kholodenko[38] (iD),
G. Khreich[11] (iD), T. Kirn[14] (iD), V.S. Kirsebom[44] (iD), O. Kitouni[59] (iD), S. Klaver[33] (iD),
N. Kleijne[29,q] (iD), K. Klimaszewski[36] (iD), M.R. Kmiec[36] (iD), S. Koliiev[47] (iD), L. Kolk[15] (iD),
A. Kondybayeva[38] (iD), A. Konoplyannikov[38] (iD), P. Kopciewicz[34] (iD), R. Kopecna[17],
P. Koppenburg[32] (iD), M. Korolev[38] (iD), I. Kostiuk[32] (iD), O. Kot[47], S. Kotriakhova (iD),

A. Kozachuk[38], P. Kravchenko[38], L. Kravchuk[38], M. Kreps[51], S. Kretzschmar[14],
P. Krokovny[38], W. Krupa[34], W. Krzemien[36], J. Kubat[17], S. Kubis[76],
W. Kucewicz[35], M. Kucharczyk[35], V. Kudryavtsev[38], E.K Kulikova[38], A. Kupsc[77],
D. Lacarrere[43], G. Lafferty[57], A. Lai[27], A. Lampis[27,h], D. Lancierini[45],
C. Landesa Gomez[41], J.J. Lane[57], R. Lane[49], C. Langenbruch[14], J. Langer[15],
O. Lantwin[38], T. Latham[51], F. Lazzari[29,r], C. Lazzeroni[48], R. Le Gac[10],
S.H. Lee[78], R. Lefèvre[9], A. Leflat[38], S. Legotin[38], P. Lenisa[i,21], O. Leroy[10],
T. Lesiak[35], B. Leverington[17], A. Li[3], H. Li[67], K. Li[7], P. Li[43], P.-R. Li[68],
S. Li[7], T. Li[4], T. Li[67], Y. Li[4], Z. Li[63], X. Liang[63], C. Lin[6], T. Lin[52],
R. Lindner[43], V. Lisovskyi[15], R. Litvinov[27,h], G. Liu[67], H. Liu[6], K. Liu[68],
Q. Liu[6], S. Liu[4,6], A. Lobo Salvia[40], A. Loi[27], R. Lollini[73], J. Lomba Castro[41],
I. Longstaff[54], J.H. Lopes[2], A. Lopez Huertas[40], S. López Soliño[41], G.H. Lovell[50],
Y. Lu[4,b], C. Lucarelli[22,j], D. Lucchesi[28,o], S. Luchuk[38], M. Lucio Martinez[75],
V. Lukashenko[32,47], Y. Luo[3], A. Lupato[57], E. Luppi[21,i], K. Lynch[18], X.-R. Lyu[6],
R. Ma[6], S. Maccolini[15], F. Machefert[11], F. Maciuc[37], I. Mackay[58], V. Macko[44],
L.R. Madhan Mohan[50], A. Maevskiy[38], D. Maisuzenko[38], M.W. Majewski[34],
J.J. Malczewski[35], S. Malde[58], B. Malecki[35,43], A. Malinin[38], T. Maltsev[38],
G. Manca[27,h], G. Mancinelli[10], C. Mancuso[11,25,l], R. Manera Escalero[40],
D. Manuzzi[20], C.A. Manzari[45], D. Marangotto[25,l], J.F. Marchand[8], U. Marconi[20],
S. Mariani[43], C. Marin Benito[40], J. Marks[17], A.M. Marshall[49], P.J. Marshall[55],
G. Martelli[73,p], G. Martellotti[30], L. Martinazzoli[43,m], M. Martinelli[26,m],
D. Martinez Santos[41], F. Martinez Vidal[42], A. Massafferri[1], M. Materok[14],
R. Matev[43], A. Mathad[45], V. Matiunin[38], C. Matteuzzi[63,26], K.R. Mattioli[12],
A. Mauri[56], E. Maurice[12], J. Mauricio[40], M. Mazurek[43], M. McCann[56],
L. Mcconnell[18], T.H. McGrath[57], N.T. McHugh[54], A. McNab[57], R. McNulty[18],
B. Meadows[60], G. Meier[15], D. Melnychuk[36], S. Meloni[26,m], M. Merk[32,75],
A. Merli[25,l], L. Meyer Garcia[2], D. Miao[4,6], H. Miao[6], M. Mikhasenko[71,d],
D.A. Milanes[70], M. Milovanovic[43], M.-N. Minard[8,†], A. Minotti[26,m], E. Minucci[63],
T. Miralles[9], S.E. Mitchell[53], B. Mitreska[15], D.S. Mitzel[15], A. Modak[52],
A. Mödden [15], R.A. Mohammed[58], R.D. Moise[14], S. Mokhnenko[38],
T. Mombächer[41], M. Monk[51,64], I.A. Monroy[70], S. Monteil[9], G. Morello[23],
M.J. Morello[29,q], M.P. Morgenthaler[17], J. Moron[34], A.B. Morris[43], A.G. Morris[10],
R. Mountain[63], H. Mu[3], E. Muhammad[51], F. Muheim[53], M. Mulder[74],
K. Müller[45], D. Murray[57], R. Murta[56], P. Muzzetto[27,h], P. Naik[49], T. Nakada[44],
R. Nandakumar[52], T. Nanut[43], I. Nasteva[2], M. Needham[53], N. Neri[25,l],
S. Neubert[71], N. Neufeld[43], P. Neustroev[38], R. Newcombe[56], J. Nicolini[15,11],
D. Nicotra[75], E.M. Niel[44], S. Nieswand[14], N. Nikitin[38], N.S. Nolte[59],
C. Normand[8,h,27], J. Novoa Fernandez[41], G.N Nowak[60], C. Nunez[78],
A. Oblakowska-Mucha[34], V. Obraztsov[38], T. Oeser[14], S. Okamura[21,i],
R. Oldeman[27,h], F. Oliva[53], C.J.G. Onderwater[74], R.H. O'Neil[53],
J.M. Otalora Goicochea[2], T. Ovsiannikova[38], P. Owen[45], A. Oyanguren[42],
O. Ozcelik[53], K.O. Padeken[71], B. Pagare[51], P.R. Pais[43], T. Pajero[58],
A. Palano[19], M. Palutan[23], G. Panshin[38], L. Paolucci[51], A. Papanestis[52],
M. Pappagallo[19,f], L.L. Pappalardo[21,i], C. Pappenheimer[60], W. Parker[61],
C. Parkes[57], B. Passalacqua[21], G. Passaleva[22], A. Pastore[19], M. Patel[56],
C. Patrignani[20,g], C.J. Pawley[75], A. Pellegrino[32], M. Pepe Altarelli[43],
S. Perazzini[20], D. Pereima[38], A. Pereiro Castro[41], P. Perret[9], K. Petridis[49],
A. Petrolini[24,k], S. Petrucci[53], M. Petruzzo[25], H. Pham[63], A. Philippov[38],
R. Piandani[6], L. Pica[29,q], M. Piccini[73], B. Pietrzyk[8], G. Pietrzyk[11], D. Pinci[30],
F. Pisani[43], M. Pizzichemi[26,m,43], V. Placinta[37], J. Plews[48], M. Plo Casasus[41],

F. Polci[13,43], M. Poli Lener[23], A. Poluektov[10], N. Polukhina[38], I. Polyakov[43],
E. Polycarpo[2], S. Ponce[43], D. Popov[6,43], S. Poslavskii[38], K. Prasanth[35],
L. Promberger[17], C. Prouve[41], V. Pugatch[47], V. Puill[11], G. Punzi[29,r], H.R. Qi[3],
W. Qian[6], N. Qin[3], S. Qu[3], R. Quagliani[44], N.V. Raab[18], B. Rachwal[34],
J.H. Rademacker[49], R. Rajagopalan[63], M. Rama[29], M. Ramos Pernas[51],
M.S. Rangel[2], F. Ratnikov[38], G. Raven[33], M. Rebollo De Miguel[42], F. Redi[43],
J. Reich[49], F. Reiss[57], Z. Ren[3], P.K. Resmi[58], R. Ribatti[29,q], A.M. Ricci[27],
S. Ricciardi[52], K. Richardson[59], M. Richardson-Slipper[53], K. Rinnert[55],
P. Robbe[11], G. Robertson[53], E. Rodrigues[55,43], E. Rodriguez Fernandez[41],
J.A. Rodriguez Lopez[70], E. Rodriguez Rodriguez[41], D.L. Rolf[43], A. Rollings[58],
P. Roloff[43], V. Romanovskiy[38], M. Romero Lamas[41], A. Romero Vidal[41],
M. Rotondo[23], M.S. Rudolph[63], T. Ruf[43], R.A. Ruiz Fernandez[41], J. Ruiz Vidal[42],
A. Ryzhikov[38], J. Ryzka[34], J.J. Saborido Silva[41], N. Sagidova[38], N. Sahoo[48],
B. Saitta[27,h], M. Salomoni[43], C. Sanchez Gras[32], I. Sanderswood[42],
R. Santacesaria[30], C. Santamarina Rios[41], M. Santimaria[23], L. Santoro [1],
E. Santovetti[31], D. Saranin[38], G. Sarpis[53], M. Sarpis[71], A. Sarti[30],
C. Satriano[30,s], A. Satta[31], M. Saur[5], D. Savrina[38], H. Sazak[9],
L.G. Scantlebury Smead[58], A. Scarabotto[13], S. Schael[14], S. Scherl[55], A. M. Schertz[72], M. Schiller[54], H. Schindler[43], M. Schmelling[16], B. Schmidt[43],
S. Schmitt[14], O. Schneider[44], A. Schopper[43], M. Schubiger[32], N. Schulte[15],
S. Schulte[44], M.H. Schune[11], R. Schwemmer[43], G. Schwering[14], B. Sciascia[23],
A. Sciuccati[43], S. Sellam[41], A. Semennikov[38], M. Senghi Soares[33], A. Sergi[24,k],
N. Serra[45], L. Sestini[28], A. Seuthe[15], Y. Shang[5], D.M. Shangase[78], M. Shapkin[38],
I. Shchemerov[38], L. Shchutska[44], T. Shears[55], L. Shekhtman[38], Z. Shen[5],
S. Sheng[4,6], V. Shevchenko[38], B. Shi[6], E.B. Shields[26,m], Y. Shimizu[11],
E. Shmanin[38], R. Shorkin[38], J.D. Shupperd[63], B.G. Siddi[21,i], R. Silva Coutinho[63],
G. Simi[28], S. Simone[19,f], M. Singla[64], N. Skidmore[57], R. Skuza[17],
T. Skwarnicki[63], M.W. Slater[48], J.C. Smallwood[58], J.G. Smeaton[50], E. Smith[59],
K. Smith[62], M. Smith[56], A. Snoch[32], L. Soares Lavra[9], M.D. Sokoloff[60],
F.J.P. Soler[54], A. Solomin[38,49], A. Solovev[38], I. Solovyev[38], R. Song[64],
F.L. Souza De Almeida[2], B. Souza De Paula[2], E. Spadaro Norella[25,l], E. Spedicato[20],
J.G. Speer[15], E. Spiridenkov[38], P. Spradlin[54], V. Sriskaran[43], F. Stagni[43],
M. Stahl[43], S. Stahl[43], S. Stanislaus[58], E.N. Stein[43], O. Steinkamp[45],
O. Stenyakin[38], H. Stevens[15], D. Strekalina[38], Y.S Su[6], F. Suljik[58], J. Sun[27],
L. Sun[69], Y. Sun[61], P.N. Swallow[48], K. Swientek[34], A. Szabelski[36], T. Szumlak[34],
M. Szymanski[43], Y. Tan[3], S. Taneja[57], M.D. Tat[58], A. Terentev[45], F. Teubert[43],
E. Thomas[43], D.J.D. Thompson[48], H. Tilquin[56], V. Tisserand[9], S. T'Jampens[8],
M. Tobin[4], L. Tomassetti[21,i], G. Tonani[25,l], X. Tong[5], D. Torres Machado[1],
L. Toscano[15], D.Y. Tou[3], C. Trippl[44], G. Tuci[17], N. Tuning[32], A. Ukleja[36],
D.J. Unverzagt[17], A. Usachov[33], A. Ustyuzhanin[38], U. Uwer[17], V. Vagnoni[20],
A. Valassi[43], G. Valenti[20], N. Valls Canudas[39], M. Van Dijk[44], H. Van Hecke[62],
E. van Herwijnen[56], C.B. Van Hulse[41,v], M. van Veghel[32], R. Vazquez Gomez[40],
P. Vazquez Regueiro[41], C. Vázquez Sierra[41], S. Vecchi[21], J.J. Velthuis[49],
M. Veltri[22,u], A. Venkateswaran[44], M. Vesterinen[51], D. Vieira[60], M. Vieites Diaz[44],
X. Vilasis-Cardona[39], E. Vilella Figueras[55], A. Villa[20], P. Vincent[13], F.C. Volle[11],
D. vom Bruch[10], V. Vorobyev[38], N. Voropaev[38], K. Vos[75], C. Vrahas[53], J. Walsh[29],
E.J. Walton[64], G. Wan[5], C. Wang[17], G. Wang[7], J. Wang[5], J. Wang[4],
J. Wang[3], J. Wang[69], M. Wang[25], R. Wang[49], X. Wang[67], Y. Wang[7],
Z. Wang[45], Z. Wang[3], Z. Wang[6], J.A. Ward[51,64], N.K. Watson[48], D. Websdale[56],
Y. Wei[5], B.D.C. Westhenry[49], D.J. White[57], M. Whitehead[54], A.R. Wiederhold[51],

27

D. Wiedner[15] ⬡, G. Wilkinson[58] ⬡, M.K. Wilkinson[60] ⬡, I. Williams[50], M. Williams[59] ⬡,
M.R.J. Williams[53] ⬡, R. Williams[50] ⬡, F.F. Wilson[52] ⬡, W. Wislicki[36] ⬡, M. Witek[35] ⬡,
L. Witola[17] ⬡, C.P. Wong[62] ⬡, G. Wormser[11] ⬡, S.A. Wotton[50] ⬡, H. Wu[63] ⬡, J. Wu[7] ⬡,
Y. Wu[5] ⬡, K. Wyllie[43] ⬡, Z. Xiang[6] ⬡, Y. Xie[7] ⬡, A. Xu[5] ⬡, J. Xu[6] ⬡, L. Xu[3], L. Xu[3] ⬡,
M. Xu[51] ⬡, Q. Xu[6], Z. Xu[9] ⬡, Z. Xu[6] ⬡, Z. Xu[4] ⬡, D. Yang[3] ⬡, S. Yang[6] ⬡, X. Yang[5] ⬡,
Y. Yang[6] ⬡, Z. Yang[5] ⬡, Z. Yang[61] ⬡, V. Yeroshenko[11] ⬡, H. Yeung[57] ⬡, H. Yin[7] ⬡,
J. Yu[66] ⬡, X. Yuan[63] ⬡, E. Zaffaroni[44] ⬡, M. Zavertyaev[16] ⬡, M. Zdybal[35] ⬡, M. Zeng[3] ⬡,
C. Zhang[5] ⬡, D. Zhang[7] ⬡, J. Zhang[6] ⬡, L. Zhang[3] ⬡, S. Zhang[66] ⬡, S. Zhang[5] ⬡,
Y. Zhang[5] ⬡, Y. Zhang[58], Y. Zhao[17] ⬡, A. Zharkova[38] ⬡, A. Zhelezov[17] ⬡, Y. Zheng[6] ⬡,
T. Zhou[5] ⬡, X. Zhou[7] ⬡, Y. Zhou[6] ⬡, V. Zhovkovska[11] ⬡, X. Zhu[3] ⬡, X. Zhu[7] ⬡, Z. Zhu[6] ⬡,
V. Zhukov[14,38] ⬡, J. Zhuo[42] ⬡, Q. Zou[4,6] ⬡, S. Zucchelli[20,g] ⬡, D. Zuliani[28] ⬡, G. Zunica[57] ⬡.

[1]Centro Brasileiro de Pesquisas Físicas (CBPF), Rio de Janeiro, Brazil
[2]Universidade Federal do Rio de Janeiro (UFRJ), Rio de Janeiro, Brazil
[3]Center for High Energy Physics, Tsinghua University, Beijing, China
[4]Institute Of High Energy Physics (IHEP), Beijing, China
[5]School of Physics State Key Laboratory of Nuclear Physics and Technology, Peking University, Beijing, China
[6]University of Chinese Academy of Sciences, Beijing, China
[7]Institute of Particle Physics, Central China Normal University, Wuhan, Hubei, China
[8]Université Savoie Mont Blanc, CNRS, IN2P3-LAPP, Annecy, France
[9]Université Clermont Auvergne, CNRS/IN2P3, LPC, Clermont-Ferrand, France
[10]Aix Marseille Univ, CNRS/IN2P3, CPPM, Marseille, France
[11]Université Paris-Saclay, CNRS/IN2P3, IJCLab, Orsay, France
[12]Laboratoire Leprince-Ringuet, CNRS/IN2P3, Ecole Polytechnique, Institut Polytechnique de Paris, Palaiseau, France
[13]LPNHE, Sorbonne Université, Paris Diderot Sorbonne Paris Cité, CNRS/IN2P3, Paris, France
[14]I. Physikalisches Institut, RWTH Aachen University, Aachen, Germany
[15]Fakultät Physik, Technische Universität Dortmund, Dortmund, Germany
[16]Max-Planck-Institut für Kernphysik (MPIK), Heidelberg, Germany
[17]Physikalisches Institut, Ruprecht-Karls-Universität Heidelberg, Heidelberg, Germany
[18]School of Physics, University College Dublin, Dublin, Ireland
[19]INFN Sezione di Bari, Bari, Italy
[20]INFN Sezione di Bologna, Bologna, Italy
[21]INFN Sezione di Ferrara, Ferrara, Italy
[22]INFN Sezione di Firenze, Firenze, Italy
[23]INFN Laboratori Nazionali di Frascati, Frascati, Italy
[24]INFN Sezione di Genova, Genova, Italy
[25]INFN Sezione di Milano, Milano, Italy
[26]INFN Sezione di Milano-Bicocca, Milano, Italy
[27]INFN Sezione di Cagliari, Monserrato, Italy
[28]Università degli Studi di Padova, Università e INFN, Padova, Padova, Italy
[29]INFN Sezione di Pisa, Pisa, Italy
[30]INFN Sezione di Roma La Sapienza, Roma, Italy
[31]INFN Sezione di Roma Tor Vergata, Roma, Italy
[32]Nikhef National Institute for Subatomic Physics, Amsterdam, Netherlands
[33]Nikhef National Institute for Subatomic Physics and VU University Amsterdam, Amsterdam, Netherlands
[34]AGH - University of Science and Technology, Faculty of Physics and Applied Computer Science, Kraków, Poland
[35]Henryk Niewodniczanski Institute of Nuclear Physics Polish Academy of Sciences, Kraków, Poland
[36]National Center for Nuclear Research (NCBJ), Warsaw, Poland
[37]Horia Hulubei National Institute of Physics and Nuclear Engineering, Bucharest-Magurele, Romania
[38]Affiliated with an institute covered by a cooperation agreement with CERN
[39]DS4DS, La Salle, Universitat Ramon Llull, Barcelona, Spain

[40] *ICCUB, Universitat de Barcelona, Barcelona, Spain*

[41] *Instituto Galego de Física de Altas Enerxías (IGFAE), Universidade de Santiago de Compostela, Santiago de Compostela, Spain*

[42] *Instituto de Fisica Corpuscular, Centro Mixto Universidad de Valencia - CSIC, Valencia, Spain*

[43] *European Organization for Nuclear Research (CERN), Geneva, Switzerland*

[44] *Institute of Physics, Ecole Polytechnique Fédérale de Lausanne (EPFL), Lausanne, Switzerland*

[45] *Physik-Institut, Universität Zürich, Zürich, Switzerland*

[46] *NSC Kharkiv Institute of Physics and Technology (NSC KIPT), Kharkiv, Ukraine*

[47] *Institute for Nuclear Research of the National Academy of Sciences (KINR), Kyiv, Ukraine*

[48] *University of Birmingham, Birmingham, United Kingdom*

[49] *H.H. Wills Physics Laboratory, University of Bristol, Bristol, United Kingdom*

[50] *Cavendish Laboratory, University of Cambridge, Cambridge, United Kingdom*

[51] *Department of Physics, University of Warwick, Coventry, United Kingdom*

[52] *STFC Rutherford Appleton Laboratory, Didcot, United Kingdom*

[53] *School of Physics and Astronomy, University of Edinburgh, Edinburgh, United Kingdom*

[54] *School of Physics and Astronomy, University of Glasgow, Glasgow, United Kingdom*

[55] *Oliver Lodge Laboratory, University of Liverpool, Liverpool, United Kingdom*

[56] *Imperial College London, London, United Kingdom*

[57] *Department of Physics and Astronomy, University of Manchester, Manchester, United Kingdom*

[58] *Department of Physics, University of Oxford, Oxford, United Kingdom*

[59] *Massachusetts Institute of Technology, Cambridge, MA, United States*

[60] *University of Cincinnati, Cincinnati, OH, United States*

[61] *University of Maryland, College Park, MD, United States*

[62] *Los Alamos National Laboratory (LANL), Los Alamos, NM, United States*

[63] *Syracuse University, Syracuse, NY, United States*

[64] *School of Physics and Astronomy, Monash University, Melbourne, Australia, associated to [51]*

[65] *Pontifícia Universidade Católica do Rio de Janeiro (PUC-Rio), Rio de Janeiro, Brazil, associated to [2]*

[66] *Physics and Micro Electronic College, Hunan University, Changsha City, China, associated to [7]*

[67] *Guangdong Provincial Key Laboratory of Nuclear Science, Guangdong-Hong Kong Joint Laboratory of Quantum Matter, Institute of Quantum Matter, South China Normal University, Guangzhou, China, associated to [3]*

[68] *Lanzhou University, Lanzhou, China, associated to [4]*

[69] *School of Physics and Technology, Wuhan University, Wuhan, China, associated to [3]*

[70] *Departamento de Fisica , Universidad Nacional de Colombia, Bogota, Colombia, associated to [13]*

[71] *Universität Bonn - Helmholtz-Institut für Strahlen und Kernphysik, Bonn, Germany, associated to [17]*

[72] *Eotvos Lorand University, Budapest, Hungary, associated to [43]*

[73] *INFN Sezione di Perugia, Perugia, Italy, associated to [21]*

[74] *Van Swinderen Institute, University of Groningen, Groningen, Netherlands, associated to [32]*

[75] *Universiteit Maastricht, Maastricht, Netherlands, associated to [32]*

[76] *Faculty of Material Engineering and Physics, Cracow, Poland, associated to [35]*

[77] *Department of Physics and Astronomy, Uppsala University, Uppsala, Sweden, associated to [54]*

[78] *University of Michigan, Ann Arbor, MI, United States, associated to [63]*

[a] *Universidade de Brasília, Brasília, Brazil*

[b] *Central South U., Changsha, China*

[c] *Hangzhou Institute for Advanced Study, UCAS, Hangzhou, China*

[d] *Excellence Cluster ORIGINS, Munich, Germany*

[e] *Universidad Nacional Autónoma de Honduras, Tegucigalpa, Honduras*

[f] *Università di Bari, Bari, Italy*

[g] *Università di Bologna, Bologna, Italy*

[h] *Università di Cagliari, Cagliari, Italy*

[i] *Università di Ferrara, Ferrara, Italy*

[j] *Università di Firenze, Firenze, Italy*

[k] *Università di Genova, Genova, Italy*

[l] *Università degli Studi di Milano, Milano, Italy*

[m] *Università di Milano Bicocca, Milano, Italy*

[n] *Università di Modena e Reggio Emilia, Modena, Italy*

[o]Università di Padova, Padova, Italy

[p]Università di Perugia, Perugia, Italy

[q]Scuola Normale Superiore, Pisa, Italy

[r]Università di Pisa, Pisa, Italy

[s]Università della Basilicata, Potenza, Italy

[t]Università di Roma Tor Vergata, Roma, Italy

[u]Università di Urbino, Urbino, Italy

[v]Universidad de Alcalá, Alcalá de Henares , Spain

[w]Universidade da Coruña, Coruña, Spain

[†]Deceased